The mechanisms for elevation of serum levels of proinflammatory molecules in type 2 diabetes remain unclear, although it might be at least partially caused by oxidative stress [9]. Activation of nuclear factor-κB through oxidative stress-induced by hyperglycemia increases concentrations of circulating proinflammatory cytokines [10].

We previously demonstrated that leukocyte adhesion molecules including E-selectin and P-selectin are up-regulated in the kidney of diabetic patients [11]. We also reported that intercellular adhesion molecules (ICAM)-1 is up-regulated in the kidney of experimental diabetic rats and mediates infiltration of macrophages into diabetic kidney [12]. In another report, serum level of vascular cell adhesion molecules (VCAM)-1 is elevated in diabetic patients [13]. Moreover, macrophage infiltration and renal injuries were prevented in ICAM-1 deficient mice after induction of diabetes [14]. These findings suggest that inflammatory process is also involved in the pathogenesis of diabetic nephropathy.

We have recently reported that serum level of IL-18 is positively correlated with urinary albumin excretion, brachial-ankle pulse wave velocity (baPWV) and intima media thickness of carotid artery (IMT) and both serum and urinary levels of IL-18 are independently correlated with urinary albumin excretion rate (AER) [15]. These findings suggest that IL-18 might be a predictor of progression of diabetic nephropathy as well as atherosclerosis. Elevated level of fibrinogen, an independent risk factor for cardiovascular disease, is also associated with AER [16]. These findings suggest that inflammatory process is involved in both atherosclerosis and diabetic nephropathy. Proinflammatory cytokines, chemokines and adhesion molecules may compose a complex network and contribute to the progression of vascular complications in diabetic patients.

The aim of this study is to evaluate the change of serum profile of proinflammatory molecules including cytokines, chemokines and adhesion molecules in patients with type 2 diabetes and clarify the involvement of these molecules in diabetic nephropathy and atherosclerosis.

2. Subjects, materials and methods

2.1. Study population

A total of 66 Japanese patients (32 females and 34 males) with type 2 diabetes were enrolled in this study. All patients were fulfilled the following inclusion criteria; initially diagnosed diabetes at over 40 of their age, negative about antibody to GAD, no history of ketoacidosis, no renal insufficiency (creatinine clearance >1.00 ml/s), never received any hormone replacement therapy. Cardiovascular disease was defined as an attack of stroke, ischemic heart disease and arteriosclerosis obliterans. Their mean age was 61.0 ± 7.8 (mean ± SD), diabetic duration 10.4 ± 6.4 years, BMI 23.9 ± 3.2 kg/m^2, HbA_{1c} 7.3 ± 1.2%.

A total of 39 age and sex matched healthy adults (24 females and 15 males) were enrolled as control subjects. Inclusion criteria for control subjects was as follows; never diagnosed diabetes, fasting plasma glucose <6.1 mmol/l, HbA_{1c} <5.8%, blood pressure <140/90 mmHg, AER <30 mg/gCr, creatinine clearance >1.00 ml/s, no medication or treatment. Their mean age was 58.1 ± 7.6, BMI 22.1 ± 2.3 kg/m^2, HbA_{1c} 5.1 ± 0.5%.

Informed consent was obtained from all participants and control subjects, and this study was approved by the Ethical Committee of Okayama Saiseikai General Hospital.

2.2. Collection of blood and urine samples

Collection of blood and urine samples was performed in the early morning after overnight fast. Creatinine clearance was determined using Cockcroft-Gault formula. AER was determined with immunoturbidimetric assay Micro Alb (Nitto Boseki Co., Ltd, Tokyo, Japan). Normoalbuminuria was defined as AER 30 mg/gCr, microalubminuria was defined as AER 30–299 mg/gCr and macroalbuminuria was defined as AER >300 mg/gCr. Blood and urine samples were centrifuged immediately after collection and the supernatants were stored at −80 °C and −30 °C until analysis, respectively. All samples were measured at one time after sample collection.

2.3. Measurements of serum proinflammatory molecules

Serum levels of IL-6 were measured using a chemiluminescent enzyme assay (CLEIA kit; Fujirebio, Tokyo, Japan). Serum levels of high-sensitivity (hs) TNF-α, IP-10, monocyte chemotactic protein (MCP)-1, ICAM-1, VCAM-1, E-selectin and L-selectin were measured using a quantitative sandwich enzyme immunoassay (R&D Systems, Minneapolis, USA). Serum P-selectin was measured using an enzyme-linked immunosorbent assay (TaKaRa, Kyoto, Japan).

2.4. Measurements of carotid IMT and baPWV

IMT of the common carotid artery was determined using duplex ultrasonography with a 7.5 MHz linear transducer (SSD-5500; Aloka, Tokyo, Japan). As we previously referred [15], carotid IMT was defined as the distance from the leading edge of the first echogenic line to the second echogenic line on a sonographic image. Measurements of IMT were made at each of the three sites of the greatest thickness on both sides. The mean of these maximal IMT measurements was used for analysis.

Systolic blood pressure (SBP) and diastolic blood pressure (DBP) were measured twice with the patient in a sitting position after 5 min rest. Left and right baPWV was measured automatically using an ABI-form (BP-203RPE II; Nippon Colin, Komaki, Japan). A trained physician at Okayama Saiseikai General Hospital performed all scans. In this study, the highest values of SBP, DBP, IMT and baPWV from the left and the right sides were used for the evaluation of each patient.

2.5. Statistics

All statistical analysis was performed by SPSS for Windows statistical software system. All data are represented as mean ± SD or actual numbers. Comparison of data between type 2 diabetic patients and control subjects was evaluated using unpaired Student's t-test and χ^2 for sex. AER, hsCRP, IL-6, hsTNF-α, IP-10, MCP-1, ICAM-1, VCAM-1, P-selectin, E-selectin and L-selectin were not normally distributed (Shapiro–Wilkes test) and natural logarithmic transformation was used to shift

the variables into normal distribution. Correlation was evaluated using univariate and multivariate linear regression analysis. A value of $P < 0.05$ was considered to be statistically significant.

3. Results

3.1. *Clinical characteristics and serum levels of proinflammatory molecules in diabetic patients and control subjects*

Clinical characteristics and serum levels of proinflammatory molecules between type 2 diabetic patients and control subjects were shown in Table 1. BMI, HDL-cholesterol, fibrinogen, hsCRP in type 2 diabetic patients were significantly higher than in control subjects. As for blood pressure, no significant valiance was observed between type 2 diabetic patients and control subjects. In type 2 diabetic patients, the number of patients with normoalbuminuria, microalbuminuria and macroalbuminuria was 42, 18 and 6, respectively. AER, baPWV and IMT in type 2 diabetic patients were significantly higher than in control subjects (AER 120 ± 480 vs. 10.2 ± 10 mg/gCr, $P < 0.001$; baPWV 17.0 ± 3.5 vs. 14.7 ± 2.5 m/s, $P < 0.001$; IMT 0.86 ± 0.19 vs. 0.73 ± 0.15 mm, $P = 0.001$). There were 11 diabetic patients with episodes of cardiovascular disease. In type 2 diabetic patients, 8 patients received dietary therapy only, 31 patients received oral hypoglycemic agents and 27 patients received insulin replacement therapy. Twenty-four patients were administered angiotensin converting enzyme inhibitors or angiotensin receptor antagonists. Fourteen patients were administered statins.

Serum IL-6 levels were significantly higher in type 2 diabetic patients than in control subjects (1.92 ± 1.24 vs. 1.32 ± 0.78 pg/ml, $P = 0.005$). There was no significant difference in TNF-α levels between type 2 diabetic patients and control subjects. Serum IP-10 levels were significantly higher in type 2 diabetic patients than in control subjects (76.5 ± 37 vs. 55.7 ± 16 pg/ml, $P = 0.004$).

Table 1 – Characteristics of type 2 diabetic patients and control subjects.

	Control subjects ($n = 39$)	Diabetic patients ($n = 66$)	P-value
Sex (female) (n)	24	32	0.228
Age (years)	58.1 ± 7.6	61.0 ± 7.8	0.062
BMI (kg/m^2)	22.1 ± 2.3	23.9 ± 3.2	0.001
SBP (mmHg)	125 ± 12	130 ± 15	0.064
DBP (mmHg)	77 ± 10	77 ± 9	0.954
Fasting plasma glucose (mmol/l)	5.46 ± 0.5	8.44 ± 3.3	<0.001
HbA_{1c} (%)	5.1 ± 0.5	7.3 ± 1.2	<0.001
Creatinine clearance (ml/s)	1.53 ± 0.3	1.55 ± 0.4	0.811
Total cholesterol (mmol/l)	5.69 ± 1.0	5.37 ± 0.8	0.082
HDL-cholesterol (mmol/l)	1.57 ± 0.5	1.39 ± 0.4	0.044
LDL-cholesterol (mmol/l)	3.47 ± 0.9	3.25 ± 0.8	0.180
Triglyceride (mmol/l)	1.27 ± 0.6	1.59 ± 1.1	0.101
Fibrinogen (g/l)	2.76 ± 0.4	3.01 ± 0.5	0.013
hsCRP (mg/l)	0.054 ± 0.06	0.11 ± 0.1	–
(ln)hsCRP (ln[mg/l])	−3.28 ± 1.2	−2.69 ± 0.9	0.006
Duration of diabetes (years)	–	10.4 ± 6.4	–
History of cardiovascular events (yes) (n)	–	11	–
Albumin excretion rate (mg/gCr)	10.2 ± 10	120 ± 480	–
(ln)AER (ln[mg/gCr])	1.92 ± 0.9	2.92 ± 1.6	<0.001
baPWV (m/s)	14.7 ± 2.5	17.0 ± 3.5	<0.001
IMT (mm)	0.73 ± 0.15	0.86 ± 0.19	0.001
Serum IL-6 (pg/ml)	1.32 ± 0.78	1.92 ± 1.24	–
(ln) serum IL-6 (ln[pg/ml])	0.12 ± 0.58	0.47 ± 0.63	0.005
Serum hsTNF-α (pg/ml)	1.18 ± 0.46	1.23 ± 0.48	–
(ln) serum hsTNF-α (ln[pg/ml])	0.06 ± 0.54	0.15 ± 0.37	0.363
Serum IP-10 (pg/ml)	55.7 ± 16	76.5 ± 37	–
(ln) serum IP-10 (ln[pg/ml])	3.98 ± 0.27	4.25 ± 0.40	0.004
Serum MCP-1 (pg/ml)	213 ± 50	249 ± 57	–
(ln) serum MCP-1 (ln[pg/ml])	5.33 ± 0.26	5.49 ± 0.23	0.001
Serum ICAM-1 (ng/ml)	225 ± 66	236 ± 62.1	–
(ln) serum ICAM-1 (ln[ng/ml])	4.39 ± 0.62	5.42 ± 0.28	<0.001
Serum VCAM-1 (ng/ml)	651 ± 181	701 ± 181	–
(ln) serum VCAM-1 (ln[ng/ml])	6.44 ± 0.27	6.52 ± 0.25	0.151
Serum P-selectin (ng/ml)	230 ± 96	243 ± 119	–
(ln) serum P-selectin (ln[ng/ml])	5.33 ± 0.26	5.37 ± 0.51	0.583
Serum E-selectin (ng/ml)	45.2 ± 21	47.2 ± 18	–
(ln) serum E-selectin (ln[ng/ml])	3.72 ± 0.42	3.78 ± 0.38	0.434
Serum L-selectin (ng/ml)	863 ± 222	799 ± 208	–
(ln) serum L-selectin (ln[ng/ml])	6.73 ± 0.26	6.65 ± 0.26	0.140

Data are mean ± SD. P for type 2 diabetic subjects versus control subjects.

Table 2 – Simple correlation between logarithmic AER, baPWV or IMT and clinical characteristics and serum levels of proinflammatory molecules in Japanese type 2 diabetic patients.

Variables	(ln)AER		baPWV		IMT	
	r	P	r	P	r	P
Sex (female) (n)	0.023	0.857	0.079	0.533	0.235	0.062
Age (years)	0.222	0.073	0.627	<0.001	0.242	0.054
BMI (kg/m^2)	0.161	0.198	0.191	0.130	0.231	0.066
SBP (mmHg)	0.229	0.064	0.323	0.009	−0.006	0.960
DBP (mmHg)	0.096	0.442	0.135	0.286	0.060	0.637
Fasting plasma glucose (mmol/l)	0.187	0.133	0.032	0.803	0.045	0.721
HbA_{1c} (%)	0.282	0.022	0.199	0.115	0.184	0.145
Creatinine clearance (ml/s)	−0.081	0.519	−0.095	0.458	0.058	0.653
Total cholesterol (mmol/l)	0.046	0.715	−0.028	0.828	−0.053	0.676
HDL-cholesterol (mmol/l)	−0.120	0.343	−0.024	0.855	−0.374	0.003
LDL-cholesterol (mmol/l)	−0.012	0.923	−0.088	0.492	0.163	0.198
Triglyceride (mmol/l)	0.203	0.103	0.057	0.656	0.103	0.420
(ln) hsCRP (ln[mg/l])	0.263	0.037	0.100	0.442	0.296	0.021
(ln) serum IL-6 (ln[pg/ml])	0.020	0.874	0.013	0.920	0.298	0.017
(ln) serum hsTNF-α (ln[pg/ml])	0.329	0.010	0.307	0.018	0.332	0.011
(ln) serum IP-10 (ln[pg/ml])	0.371	0.002	0.509	<0.001	0.265	0.036
(ln) serum MCP-1 (ln[pg/ml])	0.090	0.471	0.152	0.229	0.107	0.401
(ln) serum ICAM-1 (ln[ng/ml])	0.203	0.101	0.040	0.757	−0.016	0.900
(ln) serum VCAM-1 (ln[ng/ml])	0.341	0.005	0.331	0.008	−0.028	0.826
(ln) serum P-selectin (ln[ng/ml])	0.101	0.418	0.020	0.876	0.227	0.071
(ln) serum E-selectin (ln[ng/ml])	0.444	<0.001	0.018	0.889	0.156	0.218
(ln) serum L-selectin (ln[ng/ml])	−0.004	0.973	−0.006	0.960	−0.183	0.148

Data are mean ± SD. r, simple correlation coefficient.

Serum MCP-1 levels were significantly higher in type 2 diabetic patients than in control subjects (249 ± 57 vs. 213 ± 50 pg/ml, P = 0.001). Among adhesion molecules, significant difference was observed only in ICAM-1 levels between the two groups.

3.2. *Simple correlation between AER, baPWV or IMT and clinical characteristics and serum levels of proinflammatory molecules in patients with type 2 diabetes*

We investigated simple correlation between clinical characteristics or proinflammatory molecules and AER, baPWV or IMT in type 2 diabetic patients. The correlation was shown in Table 2. A significant positive correlation between AER and HbA_{1c} (correlation coefficient [r] = 0.282, P = 0.022), serum levels of hsCRP (r = 0.263, P = 0.037), hsTNF-α (r = 0.329, P = 0.010), IP-10 (r = 0.371, P = 0.002), VCAM-1 (r = 0.341, P = 0.005) and E-selectin (r = 0.444, P < 0.001) was observed. BaPWV correlated positively with Age (r = 0.627, P < 0.001), SBP (r = 0.323, P = 0.009), serum levels of hsTNF-α (r = 0.307, P = 0.018), IP-10 (r = 0.509, P < 0.001) and VCAM-1 (r = 0.331, P = 0.008). IMT correlated positively with HDL-cholesterol (r = −0.374, P = 0.003), serum levels of hsCRP (r = 0.296, P = 0.021), IL-6 (r = 0.298, P = 0.017), hsTNF-α (r = 0.332, P = 0.011) and IP-10 (r = 0.265, P = 0.036).

As previously reported [17,18], significant simple correlation between AER, baPWV and IMT was observed both in all participants and in type 2 diabetic patients (data not shown).

3.3. *Multiple linear regression analysis of relationships between AER, baPWV or IMT and clinical characteristics and serum levels of proinflammatory molecules*

Serum levels of hsTNF-α and IP-10 were simply correlated with AER, baPWV and IMT. We next performed multiple linear regression analysis for relationships between AER, baPWV or IMT and hsTNF-α, IP-10 and clinical parameters that were significantly correlated with AER, baPWV or IMT. The correlation was shown in Table 3. Previous history of

Table 3 – Multiple linear regression analysis of relationships between AER, baPWV or IMT and clinical characteristics and serum levels of proinflammatory molecules.

Variables	β	P
Dependent variable: (ln)AER, $R^2 = 0.498$, P < 0.001		
Independent variable		
Previous history of cardiovascular events	0.549	<0.001
ln serum hsTNF-α	0.235	0.038
ln hsCRP	0.137	0.265
ln serum IP-10	0.127	0.230
HbA_{1c}	0.062	0.575
Dependent variable: baPWV, $R^2 = 0.538$, P < 0.001		
Independent variable		
Age	0.398	<0.001
SBP	0.227	0.035
Duration of diabetes	0.210	0.041
ln serum IP-10	0.209	0.047
ln serum hsTNF-α	0.118	0.260
Dependent variable: IMT, $R^2 = 0.249$, P = 0.016		
Independent variable		
ln serum IP-10	0.303	0.032
ln serum hsTNF-α	0.144	0.316
HDL-cholesterol	−0.155	0.328
ln hsCRP	0.052	0.734
ln serum IL-6	0.049	0.774

β, standard correlation coefficients; R^2, multiple coefficients of determination.

cardiovascular events (standard correlation coefficients [β] = 0.549, $P < 0.001$) and serum levels of hsTNF-α ($\beta = 0.235$, $P = 0.038$) were independently associated with AER. Age ($\beta = 0.398$, $P < 0.001$), SBP ($\beta = 0.227$, $P = 0.035$), duration of diabetes ($\beta = 0.210$, $P = 0.041$) and serum levels of IP-10 ($\beta = 0.209$, $P = 0.047$), were independently associated with baPWV. Serum levels of IP-10 ($\beta = 0.303$, $P = 0.032$) was independently associated with IMT.

4. Discussion

The current study has revealed that serum levels of various proinflammatory cytokines, chemokines and adhesion molecules associate with the severity of diabetic nephropathy and atherosclerosis. Proinflammatory molecules may compose a complex network in the kidney and atherosclerotic lesion and contribute to make pathologic lesions in diabetic patients. Our result suggests that serum levels of proinflammatory cytokines, chemokines and adhesion molecules may associate with the local change of these proinflammatory molecules in diabetic kidney and atherosclerotic lesion. Moreover, we have shown that TNF-α and IP-10 could be useful markers for the progression of diabetic nephropathy and atherosclerosis. Our data may provide important findings about the local inflammatory network in diabetic vascular complications.

Serum levels of several proinflammatory molecules were significantly increased in type 2 diabetic patients. Several reports also revealed that serum levels of these proinflammatory cytokines and chemokines were elevated in type 2 diabetic patients [19–21]. The simple correlation analysis in type 2 diabetic patients showed that both TNF-α and IP-10 significantly correlated with AER, baPWV and IMT. Moreover, in the multiple regression analysis, TNF-α was independently associated with AER and IP-10 was independently associated with baPWV and IMT. These results suggest that TNF-α strongly contributes to diabetic nephropathy and IP-10 strongly associates with atherosclerosis. Serum levels of TNF-α and VCAM-1 were not significantly higher in diabetic patients than in control subjects; however, these were correlated with AER and baPWV in type 2 diabetic patients. The age of control subjects was relatively high in our study. It might be one of the causes that the serum levels of TNF-α and VCAM-1 were similar between diabetic patients and control subjects [22].

In control subjects, simple correlation was found between serum levels of hsTNF-α and AER and between serum levels of ICAM-1 and baPWV or IMT. However, neither of these molecules was independently associated with AER, baPWV and IMT in multiple linear regression analysis (data not shown). Thus, our result might be characteristic changes in type 2 diabetic patients.

It is reported that vascular endothelial dysfunction due to oxidative stress was induced by increasing TNF-α in the coronary artery of Zucker obese fatty rats [23]. Over-expression of TNF-α was also observed in the glomeruli of streptozotocin-induced diabetic rats [24]. In another report, serum TNF-α was increased in diabetic patients with albuminuria as compared with patients without albuminuria [25]. These reports support our current finding and suggest that TNF-α contributes to glomerular injuries in diabetic patients.

IP-10 is a potent mitogenic and chemotaxic factor for vascular smooth muscle cells [4]. In the atheroma of human carotid artery, the expression of IP-10 and its receptor CXCR3 and increased invasion of T cells were observed [26]. IP-10 was also reported to participate in the formation of atherosclerotic lesions through mediating inflammatory cell invasion [4]. Taken together, elevated serum level of IP-10 may predict the increased production in atherosclerotic lesions in diabetic patients. With the view to the relationship between IP-10 and diabetic nephropathy, over-expression of IP-10 mRNA was observed in the tubulo-intestinal compartments of renal tissues from patients with diabetic nephropathy [27]. Increased IP-10 expression in the tubulo-interstitial cells was observed in the puromycin aminonucleoside (PAN) nephrosis of rats [28], which is the model of nephrotic syndrome and tubulo-intestinal nephritis. Moreover, human mesangial cells expressed CXCR3 and IP-10 stimulated proliferation of the cells [29]. These reports indicate that IP-10 might be involved in the pathogenesis of diabetic nephropathy as well as of atherosclerosis.

There was overlap in the serum levels of proinflammatory molecules and AER, baPWV and IMT between diabetic patients and control subjects in this study. There was a wide distribution of the severity of diabetic complications and atherosclerosis in diabetic participants. In addition, the sample size of our study was relatively small. Thus, this large overlap might be caused by small sample size and sample distribution. Relationships between serum proinflammatory cytokine concentrations and behavior of cytokines within target organs have remained unclear. It has also remained unclear why serum cytokines elevates in diabetic patients. Further long-term prospective study and *in vitro* analysis are required to clarify these mechanisms.

In conclusion, microinflammation may be a common risk factor for progression of atherosclerosis and diabetic nephropathy in patients with type 2 diabetes.

Conflict of interest

There are no conflicts of interest.

Acknowledgements

This study was supported in part by Grants-in-Aid for Scientific Research from the Ministry of Education, Science, Culture, Sports and Technology of Japan and Health Sciences Research Grants conducted by Ministry of Health Labor and Welfare. We thank colleagues on the medical staff at Okayama Saiseikai General Hospital who supported this study.

REFERENCES

[1] R. Ross, Atherosclerosis—an inflammatory disease, N. Engl. J. Med. 340 (1999) 115–126.

[2] J.K. Pai, T. Pischon, J. Ma, J.E. Manson, S.E. Hankinson, K. Joshipura, et al., Inflammatory markers and the risk of coronary heart disease in men and women, N. Engl. J. Med. 351 (2004) 2599–2610.
[3] J. de Jager, J.M. Dekker, A. Kooy, P.J. Kostense, G. Nijpels, R.J. Heine, et al., Endothelial dysfunction and low-grade inflammation explain much of the excess cardiovascular mortality in individuals with type 2 diabetes: the Hoorn study, Arterioscler. Thromb. Vasc. Biol. 26 (2006) 1086–1093.
[4] X. Wang, T.L. Yue, E.H. Ohlstein, C.P. Sung, G.Z. Feuerstein, Interferon-inducible protein-10 involves vascular smooth muscle cell migration, proliferation, and inflammatory response, J. Biol. Chem. 271 (1996) 24286–24293.
[5] A. Festa, R. D'Agostino, G. Howard, L. Mykkänen, R.P. Tracy, S.M. Haffner, Inflammation and microalbuminuria in nondiabetic and type 2 diabetic subjects: the insulin resistance atherosclerosis study, Kidney Int. 58 (2000) 1703–1710.
[6] J.C. Pickup, G.D. Chusney, S.M. Thomas, D. Burt, Plasma interleukin-6, tumour necrosis factor alpha and blood cytokine production in type 2 diabetes, Life Sci. 67 (2000) 291–300.
[7] A. Festa, R. D'Agostino Jr., G. Howard, L. Mykkänen, R.P. Tracy, S.M. Haffner, Chronic subclinical inflammation as part of the insulin resistance syndrome: the insulin resistance atherosclerosis study (IRAS), Circulation 102 (2000) 42–47.
[8] A.D. Pradhan, J.E. Manson, N. Rifai, J.E. Buring, P.M. Ridker, C-reactive protein, interleukin 6, and risk of developing type 2 diabetes mellitus, JAMA 286 (2001) 327–334.
[9] F. Arnalich, A. Hernanz, D. Lopez-Maderuelo, J.M. Pena, J. Camacho, R. Madero, et al., Enhanced acutephase response and oxidative stress in older adults with type II diabetes, Horm. Metab. Res. 32 (2000) 407–412.
[10] K. Esposito, F. Nappo, R. Marfella, G. Giugliano, F. Giugliano, M. Ciotola, et al., Inflammatory cytokine concentrations are acutely increased by hyperglycemia in humans: role of oxidative stress, Circulation 106 (2002) 2067–2072.
[11] K. Hirata, K. Shikata, M. Matsuda, K. Akiyama, H. Sugimoto, M. Kushiro, et al., Increased expression of selectins in kidneys of patients with diabetic nephropathy, Diabetologia 41 (1998) 185–192.
[12] H. Sugimoto, K. Shikata, K. Hirata, K. Akiyama, M. Matsuda, M. Kushiro, et al., Increased expression of intercellular adhesion molecule-1 (ICAM-1) in diabetic rat glomeruli: glomerular hyperfiltration is a potential mechanism of ICAM-1 upregulation, Diabetes 46 (1997) 2075–2081.
[13] J.P. Albertini, P. Valensi, B. Lormeau, M.H. Aurousseau, F. Ferrière, J.R. Attali, et al., Elevated concentrations of soluble E-selectin and vascular cell adhesion molecule-1 in NIDDM. Effect of intensive insulin treatment, Diabetes Care 21 (1998) 1008–1013.
[14] S. Okada, K. Shikata, M. Matsuda, D. Ogawa, H. Usui, Y. Kido, et al., Intercellular adhesion molecule-1-deficient mice are resistant against renal injury after induction of diabetes, Diabetes 52 (2003) 2586–2593.
[15] A. Nakamura, K. Shikata, M. Hiramatsu, T. Nakatou, T. Kitamura, J. Wada, et al., Serum interleukin-18 levels are associated with nephropathy and atherosclerosis in Japanese patients with type 2 diabetes, Diabetes Care 28 (2005) 2890–2985.
[16] G. Bruno, P. Cavallo-Perin, G. Bargero, M. Borra, N. D'Errico, G. Pagano, Association of fibrinogen with glycemic control and albumin excretion rate in patients with non-insulin-dependent diabetes mellitus, Ann. Intern. Med. 125 (1996) 653–657.
[17] L. Mykkanen, D. Zaccaro, D. O'Leary, G. Howard, D. Robbins, S. Haffner, Microalbuminuria and carotid artery intimamedia thickness in nondiabetic and NIDDM subjects: the insulin resistance atherosclerosis study (IRAS), Stroke 28 (1997) 1710–1716.
[18] H. Yokoyama, T. Aoki, M. Imahori, M. Kuramitsu, Subclinical atherosclerosis is increased in type 2 diabetic patients with microalbuminuria evaluated by intima-media thickness and pulse wave velocity, Kidney Int. 66 (2004) 448–454.
[19] J.F. Navarro, C. Mora, M. Gómez, M. Muros, C. López-Aguilar, J. García, Influence of renal involvement on peripheral blood mononuclear cell expression behaviour of tumour necrosis factor-alpha and interleukin-6 in type 2 diabetic patients, Nephrol. Dial. Transplant. 23 (2008) 919–926.
[20] S. Mine, Y. Okada, T. Tanikawa, C. Kawahara, T. Tabata, Y. Tanaka, Increased expression levels of monocyte CCR2 and monocyte chemoattractant protein-1 in patients with diabetes mellitus, Biochem. Biophys. Res. Commun. 344 (2006) 780–785.
[21] S. Kiyici, E. Erturk, F. Budak, C. Ersoy, E. Tuncel, C. Duran, et al., Serum monocyte chemoattractant protein-1 and monocyte adhesion molecules in type 1 diabetic patients with nephropathy, Arch. Med. Res. 37 (2006) 998–1003.
[22] L. O'Mahony, J. Holland, J. Jackson, C. Feighery, T.P. Hennessy, K. Mealy, Quantitative intracellular cytokine measurement: age-related changes in proinflammatory cytokine production, Clin. Exp. Immunol. 113 (1998) 213–219.
[23] A. Picchi, X. Gao, S. Belmadani, B.J. Potter, M. Focardi, W.M. Chilian, et al., Tumor necrosis factor-α induces endothelial dysfunction in the prediabetic metabolic syndrome, Circ. Res. 99 (2006) 69–77.
[24] H. Sugimoto, K. Shikata, J. Wada, S. Horiuchi, H. Makino, Advanced glycation end products-cytokine–nitric oxide sequence pathway in the development of diabetic nephropathy: aminoguanidine ameliorates the overexpression of tumour necrosis factor-alpha and inducible nitric oxide synthase in diabetic rat glomeruli, Diabetologia 42 (1999) 878–886.
[25] Y. Moriwaki, T. Yamamoto, Y. Shibutani, E. Aoki, Z. Tsutsumi, S. Takahashi, et al., Elevated levels of interleukin-18 and tumor necrosis factor-alpha in serum of patients with type 2 diabetes mellitus: relationship with diabetic nephropathy, Metabolism 52 (2003) 605–608.
[26] F. Mach, A. Sauty, A.S. Iarossi, G.K. Sukhova, K. Neote, P. Libby, et al., Differential expression of three T lymphocyte-activating CXC chemokines by human atheroma-associated cells, J. Clin. Invest. 104 (1999) 1041–1050.
[27] H. Schmid, A. Boucherot, Y. Yasuda, A. Henger, B. Brunner, F. Eichinger, et al., European Renal cDNA Bank (ERCB) Consortium. Modular activation of nuclear factor-kappaB transcriptional programs in human diabetic nephropathy, Diabetes 55 (2006) 2993–3003.
[28] W.W. Tang, M. Qi, J.S. Warren, G.Y. Van, Chemokine expression in experimental tubulointerstitial nephritis, J. Immunol. 159 (1997) 870–876.
[29] A. Bonacchi, P. Romagnani, R.G. Romanelli, E. Efsen, F. Annunziato, L. Lasagni, et al., Signal transduction by the chemokine receptor CXCR3: activation of Ras/ERK, Src, and phosphatidylinositol 3-kinase/Akt controls cell migration and proliferation in human vascular pericytes, J. Biol. Chem. 276 (2001) 9945–9954.

P-Selectin Glycoprotein Ligand-1 Deficiency Is Protective Against Obesity-Related Insulin Resistance

Chikage Sato,[1,2] Kenichi Shikata,[1,3] Daisho Hirota,[1] Motofumi Sasaki,[1] Shingo Nishishita,[1] Satoshi Miyamoto,[1] Ryo Kodera,[1] Daisuke Ogawa,[1,2] Atsuhito Tone,[1] Hitomi Usui Kataoka,[1] Jun Wada,[1] Nobuo Kajitani,[1] and Hirofumi Makino[1]

OBJECTIVE—An inflammatory process is involved in the mechanism of obesity-related insulin resistance. Recent studies indicate that monocyte chemoattractant protein-1 (MCP-1) is a major chemokine that promotes monocyte infiltration into adipose tissues; however, the adhesion pathway in adipose tissues remains unclear. We aimed to clarify the adhesion molecules that mediate monocyte infiltration into adipose tissue.

RESEARCH DESIGN AND METHODS—We used a DNA microarray to compare the gene expression profiles in epididymal white adipose tissues (eWAT) between *db/db* mice and C57/BL6 mice each fed a high-fat diet (HFD) or a low-fat diet (LFD). We investigated the change of insulin resistance and inflammation in eWAT in P-selectin glycoprotein ligand-1 (PSGL-1) homozygous knockout (PSGL-$1^{-/-}$) mice compared with wild-type (WT) mice fed HFD.

RESULTS—DNA microarray analysis revealed that PSGL-1, a major ligand for selectins, is upregulated in eWAT from both *db/db* mice and WT mice fed HFD. Quantitative real-time RT-PCR and immunohistochemistry showed that PSGL-1 is expressed on both endothelial cells and macrophages in eWAT of obese mice. PSGL-$1^{-/-}$ mice fed HFD showed a remarkable reduction of macrophage accumulation and expression of proinflammatory genes, including MCP-1 in eWAT. Moreover, adipocyte hypertrophy, insulin resistance, lipid metabolism, and hepatic fatty change were improved in PSGL-$1^{-/-}$ mice compared with WT mice fed HFD.

CONCLUSIONS—These results indicate that PSGL-1 is a crucial adhesion molecule for the recruitment of monocytes into adipose tissues in obese mice, making it a candidate for a novel therapeutic target for the prevention of obesity-related insulin resistance. ***Diabetes* 60:189–199, 2011**

Obesity is correlated closely with chronic low-grade inflammation in adipose tissues and insulin resistance, which causes systemic metabolic disorders (1). Accumulation of macrophages in adipose tissue is positively correlated with body weight and insulin resistance in both humans and rodents (2,3). Adipose tissue macrophages (ATMs) secrete a variety of proinflammatory cytokines and chemokines, including tumor necrosis factor (TNF)-α (4), interleukin (IL)-6, and monocyte chemoattractant protein (MCP)-1 (5), which enhance insulin resistance. ATM accumulation and insulin resistance are ameliorated in MCP-1–deficient mice (6) and C-C chemokine receptor 2 (CCR2)-deficient mice (7) fed a high-fat diet (HFD). Conversely, overexpression of MCP-1 resulted in increased numbers of ATMs along with the development of insulin resistance (6,8). These findings indicate that ATMs enhance obesity-related insulin resistance.

Monocyte infiltration into inflamed tissues is promoted by chemokines and adhesion molecules that are expressed on endothelial cells and monocytes (9). Selectin molecules and those ligands mediate leukocytes rolling along the activated endothelium, which is the first step of leukocyte recruitment into inflamed tissues. The second step is monocyte adhesion on endothelial cells mediated by intercellular adhesion molecule-1 (ICAM-1) or vascular cell adhesion molecule-1 (VCAM-1). Earlier, we reported that an inflammatory process is involved in the pathogenesis of diabetic nephropathy and that ICAM-1 deficiency is protective against the development of renal injury in diabetic mice without change of blood glucose (10–13). Several studies in humans have shown that serum levels of soluble ICAM-1 are elevated in obesity and positively correlate with central adiposity (14,15) and insulin resistance (16). Other studies have shown that serum levels of soluble E-selectin are associated with BMI or insulin resistance (17,18).

The predominant adhesion pathway of monocyte infiltration into adipose tissue is unclear. To clarify the adhesion molecules that promote monocyte infiltration into obese adipose tissue, we screened the gene expression profiles of adhesion molecules in adipose tissues from two different types of obese model mice and evaluated the functions of the candidate gene using gene knockout mice.

RESEARCH DESIGN AND METHODS

Animals and animal care. Six-week-old C57/BL6 (BL6) mice were purchased from CLEA Japan (Tokyo, Japan). The *db/db* mice (C57BL/KsJ-*db/db*) and P-selectin glycoprotein ligand-1 (PSGL-1) homozygous knockout (PSGL-$1^{-/-}$) mice on the C57/BL6J background (19,20) were purchased as 6-week-old animals from The Jackson Laboratory (Bar Harbor, ME). All mice used in this study were males and were maintained under a 12-h light/12-h dark cycle with access to food and tap water ad libitum. The animal care and all procedures were done according to the Guidelines for Animal Experimentation at Okayama University Medical School, the Japanese Government Animal Protection and Management Law (number 105), and the Japanese Government Notification on Feeding and Safekeeping of Animals (number 6).

Experimental protocol

Protocol 1. The *db/db* mice and the WT (C57/BL6) mice were fed a normal diet (Oriental Yeast, Osaka, Japan). All mice were killed at 8 weeks old, and

From the [1]Department of Medicine and Clinical Science, Okayama University Graduate School of Medicine, Dentistry and Pharmaceutical Sciences, Okayama, Japan; the [2]Department of Diabetic Nephropathy, Okayama University Graduate School of Medicine, Dentistry and Pharmaceutical Sciences, Okayama, Japan; and the [3]Center for Innovative Clinical Medicine, Okayama University Hospital, Okayama, Japan.

Corresponding author: Kenichi Shikata, shikata@md.okayama-u.ac.jp.

Received 26 December 2009 and accepted 7 October 2010. Published ahead of print at http://diabetes.diabetesjournals.org on 22 October 2010. DOI: 10.2337/db09-1894.

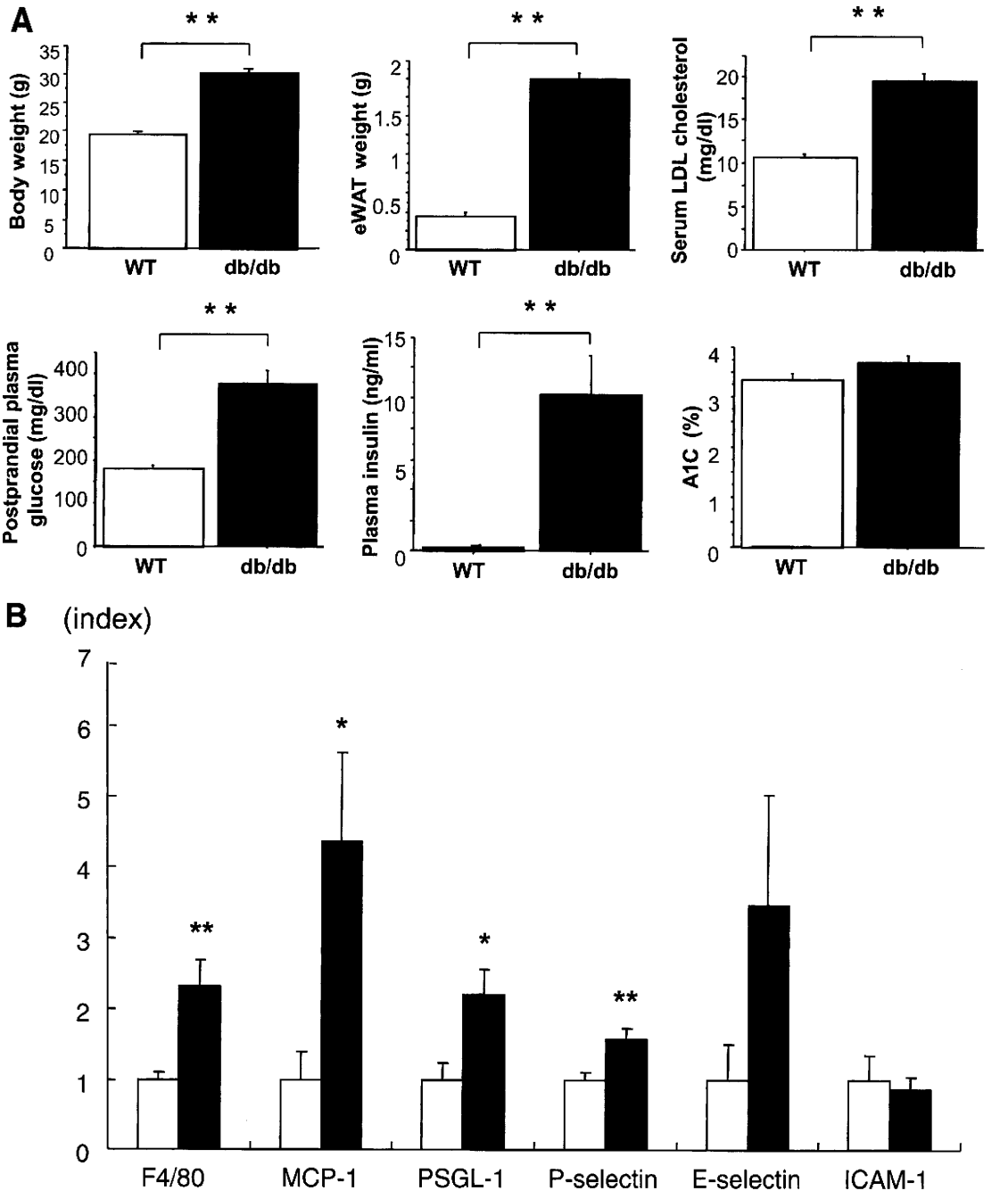

FIG. 1. *A*: Metabolic characteristics of *db/db* and WT mice. Metabolic parameters of 8-week-old WT mice (□) and *db/db* mice (■) are shown. *B*: Gene expression in epididymal fat from 8-week-old WT mice (□) and *db/db* mice (■) analyzed by quantitative real-time RT-PCR. Data are means ± SE. *$P < 0.05$, **$P < 0.005$ vs. WT. $n = 10$ for each group.

epididymal white adipose tissue (eWAT) was harvested, weighed, and fixed in 10% (vol/vol) formalin. The remaining tissue was stored at −80°C.

Protocol 2. BL6 mice were fed HFD consisting of 60% kcal fat or a low-fat diet (LFD) consisting of 10% kcal fat (D12492 and D12450B, respectively; Research Diets, New Brunswick, NJ) from 7 to 19 weeks old. Intraperitoneal glucose and insulin tolerance tests were done at 15 or 16 weeks old. All mice were killed at 19 weeks old.

Protocol 3. PSGL-$1^{-/-}$ and PSGL-$1^{+/+}$ (WT; C57/BL6) mice were fed HFD from 7 to 17 weeks old. Intraperitoneal glucose and insulin tolerance tests were done at 15 or 16 weeks old. All mice with <40 g body weight were killed at 17 weeks old. PSGL-$1^{-/-}$ mice were healthy and showed delayed neutrophil recruitment and moderate neutrophilia.

Analysis of metabolic parameters. Body weight and food intake were monitored weekly. For the glucose tolerance test, the mice were injected with glucose (1.2 g/kg body mass i.p.) after fasting for 12–16 h. For the insulin tolerance test, mice allowed access to food ad libitum were injected with human regular insulin (0.7 units/kg body mass i.p., Eli Lilly, Indianapolis, IN). We measured the concentration of glucose with a blood glucose meter (Glutest Pro; Sanwa Kagaku Kenkyusho, Nagoya, Japan), plasma insulin and leptin with an assay kit (Morinaga Institute of Biological Science, Kanagawa, Japan), and plasma adiponectin with an ELISA kit (Otsuka Pharmaceutical, Tokyo, Japan).

RNA preparation from eWAT and liver. Total RNA was extracted from each specimen of eWAT and liver using the RNeasy Lipid Tissue Mini Kit or RNeasy Plus Mini Kit following the instructions provided by the manufacturer (Qiagen, Valencia, CA).

DNA microarray analysis. We used five RNA samples from each group (*db/db* versus WT mice and BL6 mice fed HFD versus LFD) for DNA microarray analysis. Preparation of cRNA and hybridization of probe arrays (Mouse Genome 430 2.0) were performed according to the manufacturer's

TABLE 1
DNA microarray analysis

Fibulin 2	Selectin, lymphocyte
CD97 antigen	Integrin alpha x
Parvin, gamma	C-type lectin domain family 7, member a
C-type lectin domain family 4, member e	Metastasis suppressor 1
A disintegrin and metallopeptidase domain 8	Procollagen, type iii, alpha 1
Integrin alpha m	Scavenger receptor class b, member 2
Killer cell lectin-like receptor, subfamily a, member 2	Protein tyrosine phosphatase, non-receptor type substrate 1
Procollagen, type I, alpha 1	Proline-serine-threonine phosphatase-interacting protein 1
Selectin, platelet (p-selectin) ligand	Colony-stimulating factor 3 receptor (granulocyte)
Integrin alpha 7	CD36 antigen
Expressed sequence c79673	Ninjurin 1
Procollagen, type v, alpha 3	Vav 1 oncogene
Plakophilin 2	Glycoprotein (transmembrane) nmb
Elastin microfibril interfacer 2	CD22 antigen
Cell adhesion molecule with homology to l1cam	Riken cdna c030017f07 gene
Integrin beta 2	Secreted phosphoprotein 1
Milk fat globule-EGF factor 8 protein	Protocadherin 19
Pleckstrin homology, sec7 and coiled-coil domains, binding protein	Procollagen, type viii, alpha 1
CD44 antigen	Integrin beta 1 binding protein 1
Calsyntenin 2	Parvin, beta
Carboxypeptidase x 1 (m14 family)	Leupaxin
A disintegrin and metallopeptidase domain 23	Neuropilin 2
Oxidized low density lipoprotein (lectin-like) receptor 1	Complement component 1, q subcomponent, receptor 1
Procollagen, type v, alpha 2	

Gene ontology of cell adhesion category of more than twice upregulated genes *db/db* versus wild-type mice is shown (total, 47 genes).

instructions (Affymetrix, Santa Clara, CA). These arrays contain probe sets for >45,000 transcripts. The criteria for selecting genes were as follows: *1*) genes whose flags were "present" and *2*) ratio of expression level of >2.0-fold increase in *db/db* compared with WT mice or in BL6 mice fed HFD compared with LFD. Gene Ontology Biological Process classification of the >2.0-fold upregulated genes from each group was done with the DAVID Bioinformatics Database functional-annotation tools (http://niaid.abcc.ncifcrf.gov) (21).

Quantitative real-time RT-PCR analysis for eWAT and liver. The mRNA expression of each gene was measured by quantitative real-time RT-PCR as described previously (22). The amounts of PCR products were normalized with a housekeeping gene (β-actin or GAPDH) to calculate the relative expression ratios. Each experiment was done in triplicate. The primers were as follows: MCP-1: 5′-AAGCTGTAGTTTTTGTCACC-3′ (forward), 5′-GGGCA GATGCAGTTTTAA-3′ (reverse); PSGL-1 (Selpl): 5′-TTGTGCTGCTGAC CATCT-3′ (forward), 5′-TCCTCAAAATCGTCATCC-3′ (reverse); P-selectin (Selp): 5′-CAGTGGCTTCTACAACAGGC-3′ (forward), 5′-T GGGTCATATG CAGCGTTA-3′ (reverse); E-selectin (Sele): 5′-CATGGCTCAGCTCAACTT-3′ (forward), 5′-GCAGCTCATGTTCATCTT-3′ (reverse); CD68: 5′-GCGGTG GAATACAATGTG-3′ (forward), 5′-AGAGAGAGCAGGTCAAGGT-3′ (reverse); β-actin: 5′-CCTGTATGCCTCTGGTCGTA-3′ (forward), 5′-CCATCTCCTGCTC GAAGTCT-3′ (reverse).

These primers were purchased from Nihon Gene Research Labs (Sendai, Japan). ICAM-1 (GenBank accession code X52264, cat. no. 4651782) and NOS2 (iNOS) (GenBank accession code NM_010927, cat. no. 5026474) were in the Light Cycler-Primer Set (Roche Diagnostics, Rotkreuz, Switzerland). F4/80 (Mm01236959_m1), CD11c (Mm00498698_m1), IL-10 (Mm01288386_m1), IL-6 (Mm0046190_m1), LPL (Mm00434770_m1), leptin (Mm00434759_m1), fatty acid synthase (FAS) (Mm00662319_m1), sterol regulatory element binding protein-1c (SREBP-1c) (Mm0113844_m1), acetyl-CoA carboxylase-1 (ACC-1) (Mm01304289_m1), and peroxisome proliferator–activated receptor-α (PPAR-α) (Mm00627559_m1) were TaqMan gene expression assays (Applied Biosystems, Tokyo, Japan).

Isolation of adipocytes and stromal-vascular fractions. Stromal vascular fraction (SVF) cells and peripheral blood mononuclear cells (PBMCs) were isolated from *db/db* mice or BL6 mice at 10 weeks of age. SVF cells were isolated as described (23,24). PBMCs were separated by density gradient centrifugation using a Lymphocyte Separation Medium (MP Biomedicals, Solon, OH). Cells in the SVF and PBMCs were analyzed by flow cytometry.

Flow cytometry analysis. SVF cells or PBMCs were suspended in Pharmingen stain buffer (BD Biosciences, San Jose, CA) and incubated for 10 min with Fc-block and then with primary antibodies or the matching control isotypes for 30 min at 4°C. Then, the pellets were incubated with RBC Lysis Buffer (eBioscience, San Diego, CA) for 5 min and rinsed twice with Pharmingen stain buffer. After incubation with 7-amino-actinomycin D (BD Biosciences), the cells were analyzed using a FACS Calibur (BD Biosciences). Data analysis was performed using CELL Quest (BD Biosciences).

In vivo Akt phosphorylation. WT mice and PSGL-$1^{-/-}$ mice fed HFD were starved for 14 h, anesthetized with pentobarbital, and injected with 5 units of regular human insulin into the inferior vena cava. Five minutes later, the livers, eWAT, and hindlimb muscle were excised and stored at −80°C until use. Tissue samples were homogenized in RIPA Lysis buffer (Santa Cruz Biotechnology, Santa Cruz, CA) at 4°C. After centrifugation at 13,000 rpm for 30 min at 4°C, supernatant was collected. Total protein concentration was determined by using the DC-protein determination system (Bio-Rad Laboratories) and an equivalent amount of protein (40–60 μg). Samples were resolved by SDS-PAGE and transferred to a nitrocellulose membrane with iBlot Dry Blotting System (Invitrogen). The membranes were blocked with 5% nonfat dry milk in 1× Tris-buffered saline containing 0.1% Tween-20 for 1 h and incubated overnight with anti–phospho-Akt (Ser473) antibody and anti-Akt antibody (Cell Signaling Technology, Danvers, MA) at 4°C. After incubation with horseradish peroxidase–labeled secondary antibodies for 1 h, signals were detected with an enhanced chemiluminescence system (Amersham). Membranes were exposed in an Image system LAS-3000 (FujiFilm) and analyzed by using Image J software.

Light microscopy and morphometric analysis of adipocyte area. eWAT was isolated from mice, fixed in 10% formalin, and embedded in paraffin. Paraffin sections (4 μm thick) were deparaffinized and rehydrated and then stained with periodical acid Schiff stain. The adipocyte area was traced manually and analyzed with Lumina Vision OL V2.4.4 software (Mitani, Tokyo, Japan). The area was measured in six high-power fields from each of five mice.

Immunohistochemical staining. Immunoperoxidase and immunofluorescent staining were done as described (11,12,25). Paraffin sections were deparaffinized and rehydrated before antigen unmasking by boiling in R-Buffer U at a dilution of 1:10 (PickCell Laboratories, Amsterdam, the Netherlands) for 10 min.

We used immunoperoxidase staining for macrophage and PSGL-1 in eWAT of *db/db* mice and WT mice on normal food. Rat anti-mouse monocyte/macrophage (Mac-3) monoclonal antibody (mAb) at a dilution of 1:50 (Santa Cruz Biotechnology) and rat anti-mouse PSGL-1 (CD162) mAb at a dilution of 1:50 (Fitzgerald Industries International, Concord, MA) were applied to the sections as the primary reaction, followed by a second reaction with biotin-labeled donkey anti-rat IgG antibody (Jackson Immunoresearch Laboratories, West Grove, PA) at a dilution of 1:50. The avidin-biotin coupling reaction was done with the Vectastain Elite kit (Vector Laboratories, Burlingame, CA).

We used double immunofluorescence staining to clarify the expression and localization of PSGL-1, leukocyte/macrophage, and endothelial cells in eWAT of *db/db* mice. PSGL-1 mAb followed by Alexa Fluor 488 donkey anti-rat IgG (A-21208; Molecular Probes, Eugene, OR) and goat anti-mouse leukocyte/macrophage (CD45) mAb (sc-1121; Santa Cruz Biotechnology) followed by

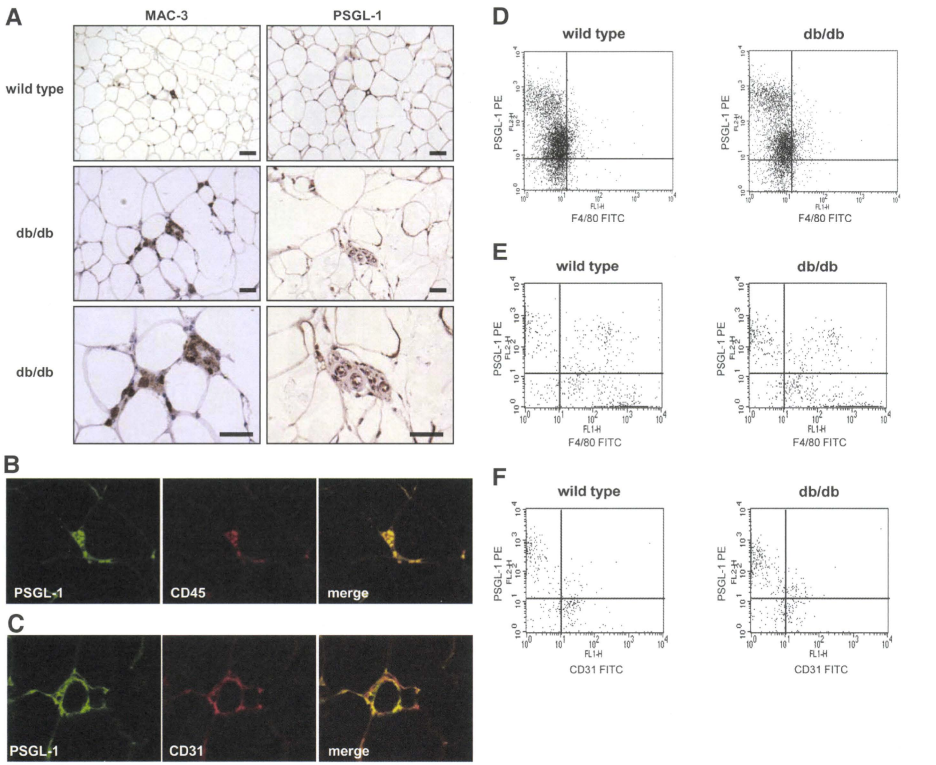

FIG. 2. *A*: **Immunohistochemical localization of PSGL-1, macrophages, and endothelial cells in adipose tissue. Epididymal fat pads from 8-week-old *db/db* mice and WT mice were stained with anti–MAC-3 (*left-hand panels*) and anti–PSGL-1 antibodies (*right-hand panels*). Macrophages and PSGL-1 expressed around the small vessels in the interstitium of adipose tissue in *db/db* mice are shown. The scale bars represent 50 μm. *B*: Double immunofluorescence staining of adipose tissue from *db/db* mice with the antibodies against PSGL-1 (*green*) and leukocyte (CD45, *red*). PSGL-1 and CD45 were stained in the interstitium of adipose tissue and are colocalized in the merged picture. *C*: Double immunofluorescence staining of adipose tissue from *db/db* mice with the antibodies against PSGL-1 (*green*) and endothelial cell (CD31, *red*). PSGL-1 and CD31 were stained along small vessels of adipose tissue and are colocalized in the merged picture. *D–F*: The expression of PSGL-1 on cells in WT mice and *db/db* mice was analyzed using flow cytometry. *D*: The expression of PSGL-1 in PBMCs. *E*: The expression of PSGL-1 in F4/80$^+$ macrophages in the SVF from adipose tissue. *F*: The expression of PSGL-1 in CD31$^+$ endothelial cells in the SVF from adipose tissue. (A high-quality digital representation of this figure is available in the online issue.)**

Alexa Fluor 546 rabbit anti-goat IgG (A-21085; Molecular Probes) were applied to the sections. Similarly, PSGL-1 mAb followed by Alexa Fluor 488 donkey anti-rat IgG and goat anti-mouse endothelial cell (PECAM-1/CD31) mAb (sc-1506; Santa Cruz Biotechnology) followed by Alexa Fluor 546 rabbit anti-goat IgG were applied to the sections.

Measurement of hepatic triglyceride content. Measurement of the hepatic triglyceride content in WT mice and PSGL-1$^{-/-}$ mice fed HFD was done by the Folch technique (26) at Skylight Biotech (Akita, Japan), and the triglyceride concentration was measured with Cholestest TG (Sekisui Medical, Tokyo, Japan). The tissue triglyceride concentrations were corrected for liver weight.

Statistical analysis. All data are expressed as mean ± SE and were analyzed by the Mann-Whitney *U* test with the level of statistical significance set at $P < 0.05$.

RESULTS

Analysis of eWAT from *db/db* mice. The *db/db* mice showed significantly increased body weight, weight of eWAT, levels of serum LDL cholesterol, postprandial plasma glucose, and plasma insulin compared with WT mice, but A1C was not different between the two groups (Fig. 1*A*).

DNA microarray analysis detected 1,080 genes that were more than twofold upregulated in *db/db* mice compared with WT mice. Gene ontology analysis indicated that 47 cell adhesion-related genes, including L-selectin (2.0-fold change, *db/db* versus wild-type) and PSGL-1 (2.0-fold change, *db/db* versus wild-type) were upregulated in *db/db* mice compared with WT mice (supplementary Fig. 1, available in an online-only appendix at http://diabetes.diabetesjournals.org/cgi/content/full/db09-1894/DC1; Table 1).

We focused on PSGL-1 because it is expressed on both

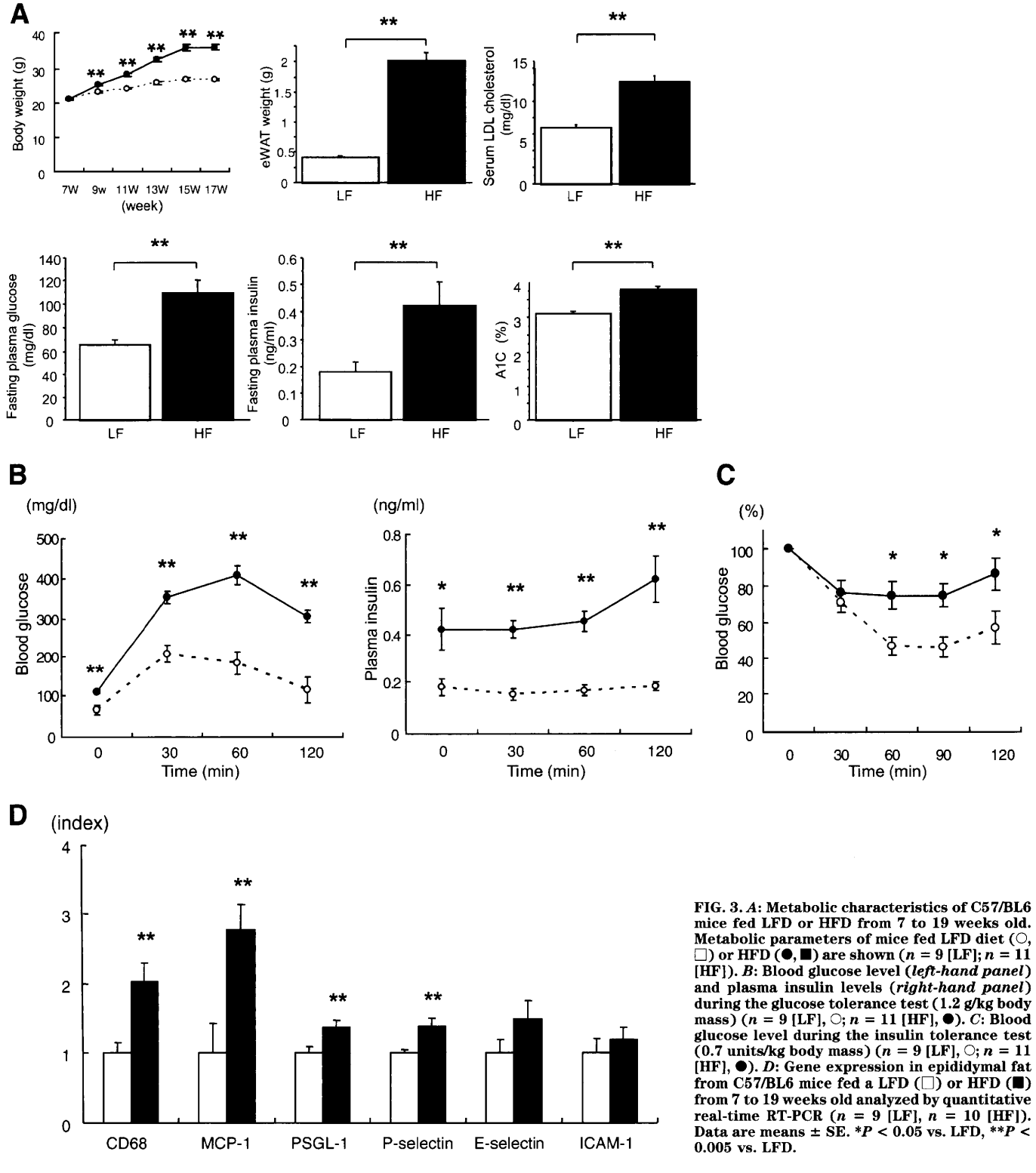

FIG. 3. *A*: **Metabolic characteristics of C57/BL6 mice fed LFD or HFD from 7 to 19 weeks old. Metabolic parameters of mice fed LFD diet (○, □) or HFD (●, ■) are shown (n = 9 [LF]; n = 11 [HF]).** *B*: **Blood glucose level (*left-hand panel*) and plasma insulin levels (*right-hand panel*) during the glucose tolerance test (1.2 g/kg body mass) (n = 9 [LF], ○; n = 11 [HF], ●).** *C*: **Blood glucose level during the insulin tolerance test (0.7 units/kg body mass) (n = 9 [LF], ○; n = 11 [HF], ●).** *D*: **Gene expression in epididymal fat from C57/BL6 mice fed a LFD (□) or HFD (■) from 7 to 19 weeks old analyzed by quantitative real-time RT-PCR (n = 9 [LF], n = 10 [HF]). Data are means ± SE. *P < 0.05 vs. LFD, **P < 0.005 vs. LFD.**

leukocytes and endothelium and has a wide range of binding capacity to all three types of selectin (27–29). Real-time RT-PCR demonstrated that PSGL-1 mRNA expression was significantly higher in eWAT of *db/db* mice compared with that in WT mice. The transcriptional levels of other proinflammatory genes, including F4/80, MCP-1, and P-selectin mRNA, were also increased significantly in *db/db* mice (Fig. 1*B*), whereas the mRNA expression of other adhesion molecule genes, such as E-selectin and ICAM-1, in *db/db* mice was not different from that in WT mice.

Immunoperoxidase staining was used for MAC-3, a macrophage marker, and PSGL-1 in eWAT from *db/db* mice and WT mice fed normal diet. The expression of macrophage and PSGL-1 increased around the small vessels in the interstitium of eWAT in *db/db* mice (Fig. 2*A*). Furthermore, to estimate the distribution of PSGL-1, macrophage, and endothelial cells in eWAT, we used double

TABLE 2
DNA microarray analysis

Connective tissue growth factor	CD44 antigen
TNF receptor superfamily, member 12a	Procollagen, type vi, alpha 3
Thrombospondin 1	Carboxypeptidase x 1 (m14 family)
Cysteine rich protein 61	Cartilage acidic protein 1
rho GTPase activating protein 6	Integrin alpha x
Procollagen, type VI, alpha 2	C-type lectin domain family 7, member a
Riken cdna 2700007f12 gene	Vav 3 oncogene
A disintegrin and metallopeptidase domain 8	Neural precursor cell expressed, developmentally downregulated gene 9
CD9 antigen	Discoidin, cub and lccl domain containing 2
Poliovirus receptor	Procollagen, type vi, alpha 1
Filamin binding lim protein 1	Periostin, osteoblast specific factor
A disintegrin and metallopeptidase domain 12 (meltrin alpha)	Protein tyrosine phosphatase, non-receptor type substrate 1
Calsyntenin 3	Proline-serine-threonine phosphatase-interacting protein 1
Poliovirus receptor-related 3	Tenascin c
Integrin alpha m	Vav 1 oncogene
Selectin, platelet (p-selectin) ligand	Glycoprotein (transmembrane) nmb
Procollagen, type I, alpha 1	Activated leukocyte cell adhesion molecule
Expressed sequence c79673	Secreted phosphoprotein 1
Immunoglobulin superfamily, member 4a	Procollagen, type viii, alpha 1
Integrin beta 2	Leupaxin
Pleckstrin homology, sec7 and coiled-coil domains, binding protein	

Gene ontology of cell adhesion category of more than twice upregulated genes HFD versus LFD is shown (total, 41 genes).

immunofluorescence staining in eWAT from *db/db* mice. PSGL-1 (*green*) and leukocyte/macrophage (CD45, *red*) were detected in the interstitium of eWAT. They were mostly coexpressed in a merged picture (Fig. 2*B*). In addition, PSGL-1 (*green*) and endothelial cells (CD31, *red*) were mostly detected in the interstitium of eWAT and mostly coexpressed in a merged picture (Fig. 2*C*).

We examined PBMCs from WT mice or *db/db* mice. $F4/80^+PSGL\text{-}1^+$ cells were similarly contained (WT mice 82.3 ± 1.2% versus *db/db* mice 84.6 ± 2.5% of $F4/80^+$ cells, $P = 0.827$) between the two groups by flow cytometry analysis. We isolated SVF cells from epididymal fat pads excised from WT mice or *db/db* mice fed a normal diet and analyzed cells by flow cytometry. $F4/80^+PSGL\text{-}1^+$ cells were not different (WT mice 23.2 ± 2.2% versus *db/db* mice 34.3 ± 4.3% of $F4/80^+$ cells, $P = 0.149$) between WT mice and *db/db* mice. $CD31^+PSGL\text{-}1^+$ cells significantly increased (WT mice 36.6 ± 2.5% versus *db/db* mice 53.9 ± 3.5% of $CD31^+$ cells, $P = 0.021$) in *db/db* mice compared with WT mice (Fig. 2*D–F*). These results indicate that $CD31^+PSGL\text{-}1^+$ cells were increased in adipose tissue of *db/db* mice.

Upregulation of PSGL-1 expression in BL6 mice fed HFD. We next examined eWAT in BL6 mice fed LFD or HFD to determine whether PSGL-1 expression increased in HFD-induced obese mice. BL6 mice fed HFD showed significantly increased body weight, weight of eWAT, serum LDL cholesterol, fasting plasma glucose, plasma insulin, and A1C compared with BL6 mice fed LFD (Fig. 3*A*). Plasma glucose and insulin levels during a glucose tolerance test were markedly higher in BL6 mice fed HFD compared with mice fed LFD (Fig. 3*B*). Similarly, BL6 mice fed HFD showed impaired insulin sensitivity as measured by the insulin tolerance test (Fig. 3*C*).

DNA microarray profiling indicated that 572 genes were upregulated more than twofold in BL6 mice fed HFD compared with those fed LFD. Analysis by gene ontology categories showed that 41 cell adhesion–related genes, including *PSGL-1*, were upregulated in BL6 mice fed HFD (twofold change, HFD/LFD) (supplementary Fig. 2, Table 2). Quantitative real-time RT-PCR showed that transcriptional levels of CD68, MCP-1, PSGL-1, and P-selectin mRNA were increased significantly in BL6 mice fed HFD. E-selectin and ICAM-1 mRNA expression were not different between the two groups (Fig. 3*D*).

PSGL-1 deficiency improved insulin sensitivity. As described above, PSGL-1 was upregulated in eWAT of two different rodent models for obesity-related insulin resistance. We further examined the role of PSGL-1 in eWAT of diet-induced obese mice using PSGL-1–deficient ($PSGL\text{-}1^{-/-}$) mice. The $PSGL\text{-}1^{-/-}$ and $PSGL\text{-}1^{+/+}$ WT mice were fed HFD for 10 weeks.

Body weight, the weight of each adipose tissue per unit body weight, and food intake were not different between the two groups (Fig. 4*A*). There was no difference in fasting plasma glucose and A1C between the two groups, although fasting plasma insulin level was significantly lower in $PSGL\text{-}1^{-/-}$ mice than it was in WT mice fed HFD (Fig. 4*B*). These data indicated that PSGL-1 deficiency improved insulin resistance without a change of body weight or the amount of eWAT.

Intraperitoneal glucose and insulin tolerance tests were used to further confirm that PSGL-1 deficiency improves insulin sensitivity. Blood glucose levels during the glucose tolerance test were similar in the two groups, although plasma insulin levels were lower in $PSGL\text{-}1^{-/-}$ mice than those in WT mice fed HFD (Fig. 4*C*). The glucose-lowering effect of insulin was significantly greater in $PSGL\text{-}1^{-/-}$ mice than it was in WT mice, as measured by the insulin tolerance test (Fig. 4*D*). These data confirmed that insulin sensitivity was improved in $PSGL\text{-}1^{-/-}$ mice fed HFD.

To further investigate insulin sensitivity in $PSGL\text{-}1^{-/-}$ mice, we examined insulin-stimulated phosphorylation of Akt in liver and muscle. Akt phosphorylation in liver was not different between the two groups. However, Akt phosphorylation in muscle was significantly increased in $PSGL\text{-}1^{-/-}$ mice compared with WT mice fed HFD (Fig. 4*E*).

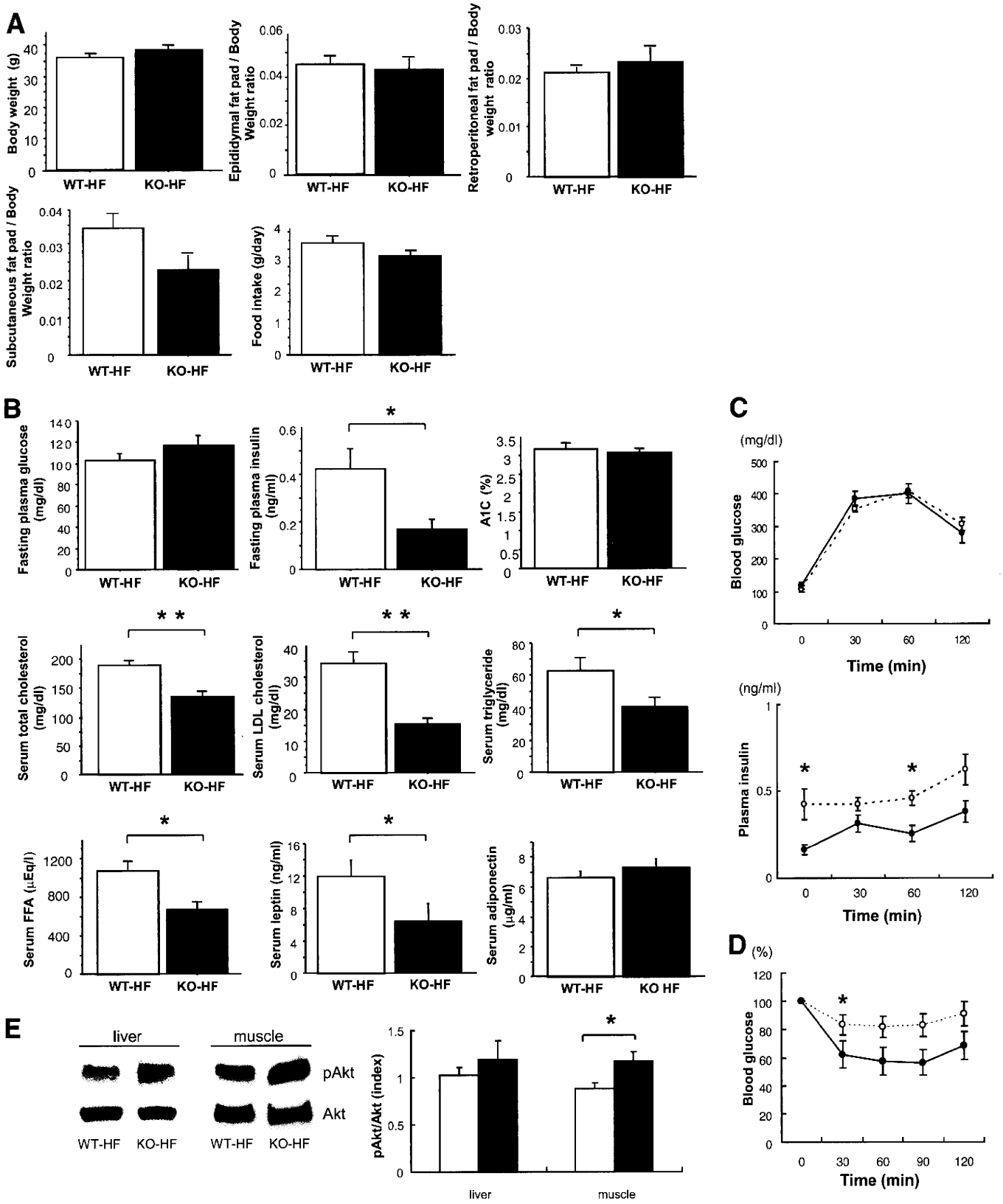

FIG. 4. *A*: **Metabolic characteristics of WT mice and PSGL-1$^{-/-}$ (KO) mice fed HFD from 7 to 17 weeks old. Body composition and food intake in WT mice (□) and PSGL-1$^{-/-}$ mice (■) fed HFD (n = 7 [WT-HF]; n = 8 [KO-HF]) is shown.** *B*: **Metabolic parameters of WT mice (□) and PSGL-1$^{-/-}$ mice (■) fed HFD (n = 7 [WT-HF]; n = 8 [KO-HF]).** *C*: **Blood glucose level (*upper panel*) and plasma insulin levels (*lower panel*) during the glucose tolerance test (1.2 g/kg body mass) (n = 9 [WT-HF], ○; n = 8 [KO-HF], ●).** *D*: **Blood glucose level during the insulin tolerance test (0.7 units/kg body mass) (n = 9 [WT-HF], ○; n = 8 [KO-HF], ●). Data are means ± SE. *P < 0.05 vs. WT-HFD, **P < 0.005 vs. WT-HFD.** *E*: **Equal amounts of protein in total lysates of liver and muscle were immunoblotted with anti–phospho-Akt (pAkt) and anti-Akt antibodies. The relative ratio of Akt phosphorylation was calculated after normalization with the Akt signal (n = 5 [WT-HF], □; n = 5 [KO-HF], ■). Data are means ± SE. *P < 0.05 vs. WT-HFD. FFA, free fatty acid.**

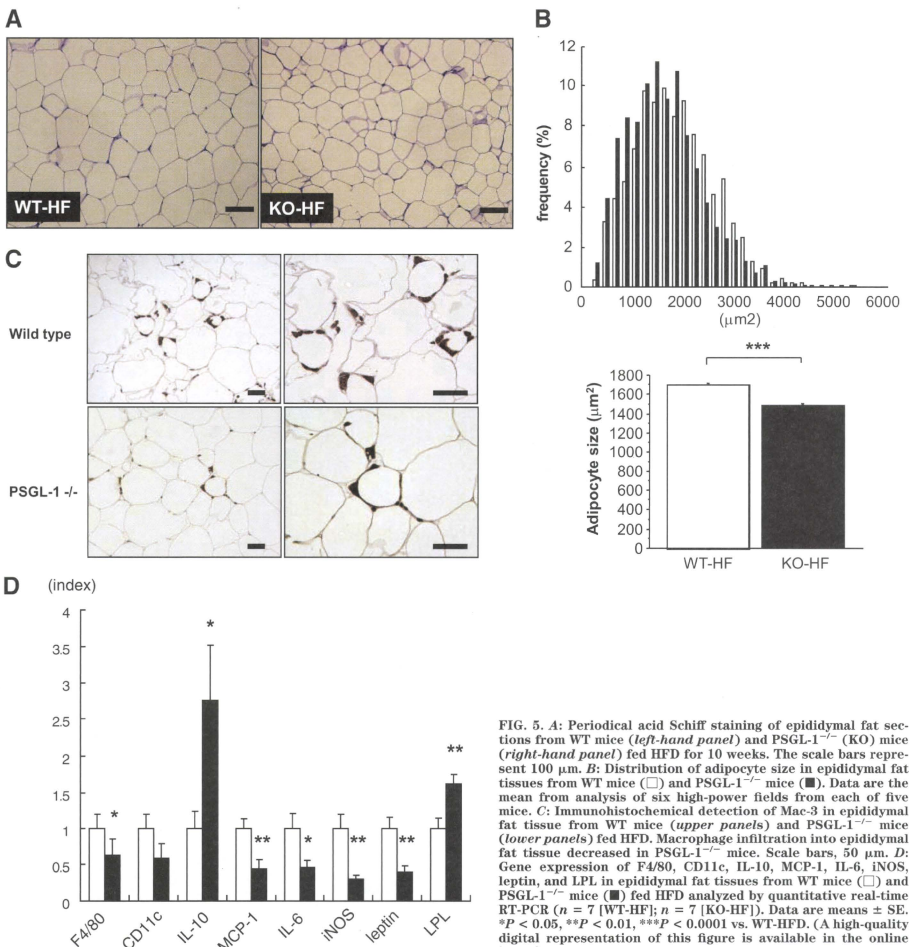

FIG. 5. *A*: **Periodical acid Schiff staining of epididymal fat sections from WT mice (*left-hand panel*) and PSGL-1$^{-/-}$ (KO) mice (*right-hand panel*) fed HFD for 10 weeks. The scale bars represent 100 μm. *B*: Distribution of adipocyte size in epididymal fat tissues from WT mice (□) and PSGL-1$^{-/-}$ mice (■). Data are the mean from analysis of six high-power fields from each of five mice. *C*: Immunohistochemical detection of Mac-3 in epididymal fat tissue from WT mice (*upper panels*) and PSGL-1$^{-/-}$ mice (*lower panels*) fed HFD. Macrophage infiltration into epididymal fat tissue decreased in PSGL-1$^{-/-}$ mice. Scale bars, 50 μm. *D*: Gene expression of F4/80, CD11c, IL-10, MCP-1, IL-6, iNOS, leptin, and LPL in epididymal fat tissues from WT mice (□) and PSGL-1$^{-/-}$ mice (■) fed HFD analyzed by quantitative real-time RT-PCR (n = 7 [WT-HF]; n = 7 [KO-HF]). Data are means ± SE. *P < 0.05, **P < 0.01, ***P < 0.0001 vs. WT-HFD. (A high-quality digital representation of this figure is available in the online issue.)**

PSGL-1 deficiency decreased macrophage infiltration and inflammation in obese adipose tissue. Morphometric analysis demonstrated that adipocytes in eWAT were smaller in PSGL-1$^{-/-}$ mice than in WT mice fed HFD (Fig. 5*A* and *B*). Immunohistochemistry showed a decrease of MAC-3–positive cells in eWAT from PSGL-1$^{-/-}$ mice fed HFD (Fig. 5*C*). The mRNA expression of F4/80, MCP-1, IL-6, iNOS, and leptin was decreased in eWAT from PSGL-1$^{-/-}$ mice compared with that in WT mice fed HFD (Fig. 5*D*), although the levels of TNF-α and adiponectin mRNA were not statistically different between the two groups (data not shown). IL-10 mRNA levels were significantly increased, whereas CD11c mRNA levels tended to be decreased without significant difference in PSGL-1$^{-/-}$ mice fed HFD compared with WT mice fed HFD (Fig. 5*D*).

PSGL-1 deficiency improved lipid metabolism and hepatic steatosis. In this study, the weight of liver and the level of serum triglycerides were reduced significantly, and the hepatic triglyceride content tended to be decreased in PSGL-1$^{-/-}$ mice compared with WT mice fed HFD (Figs. 4*B* and 6*A*). The mRNA expression of CD68 was not different between the two groups. (Fig. 6*B*). A few lipid metabolism–related genes in liver were not different between the two groups as follows: FAS (WT-HF 9.37 ± 3.07 vs. KO-HF 5.37 ± 1.38, P = 0.223), SREBP-1c (WT-HF 3.29 ± 0.48 vs. KO-HF 3.77 ± 0.64, P = 0.685), ACC-1

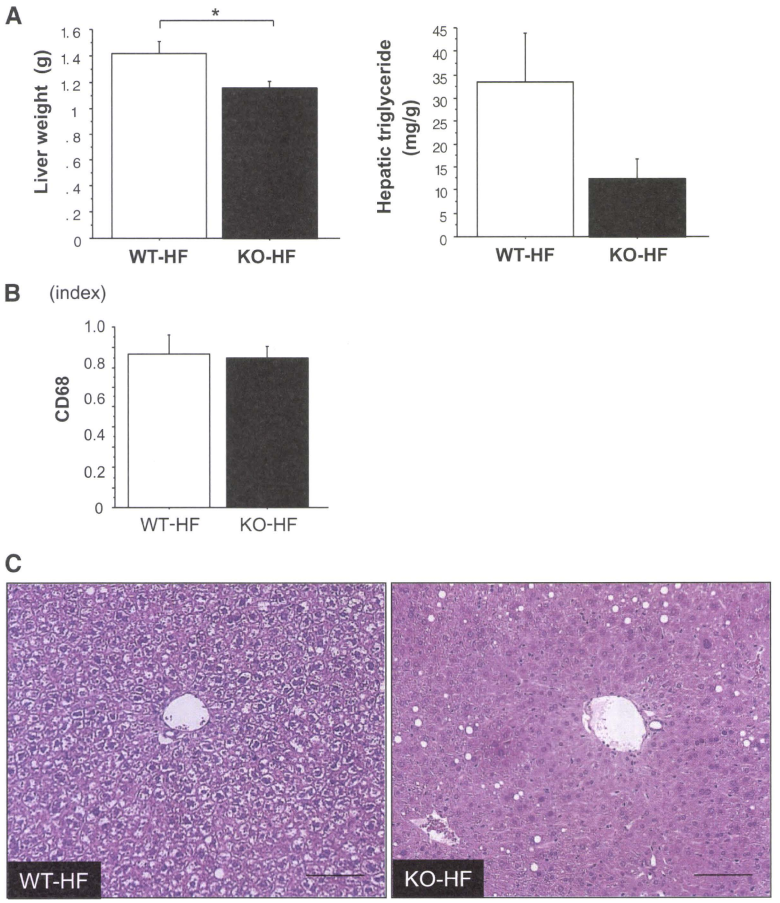

FIG. 6. *A*: **Liver weight (*left*) and hepatic triglyceride (*right*) in WT mice (□) and PSGL-1$^{-/-}$ (KO) mice (■) fed HFD for 10 weeks (n = 5 [WT-HF]; n = 8 [KO-HF]). Data are means ± SE. *P < 0.05 vs. WT-HFD. *B*: Gene expression of CD68 in liver from WT mice (□) and PSGL-1$^{-/-}$ mice (■) fed HFD diet analyzed by quantitative real-time RT-PCR (n = 5 [WT-HF]; n = 8 [KO-HF]). Data are means ± SE. *C*: Hematoxylin and eosin stain. Hepatic steatosis is prominent in the liver of WT mice fed HFD. The scale bars represent 100 μm. (A high-quality digital representation of this figure is available in the online issue.)**

(WT-HF 20.25 ± 2.63 vs. KO-HF 19.59 ± 3.09, P = 0.935), PPAR-α (WT-HF 24.45 ± 5.25 vs. KO-HF 22.93 ± 4.03, P = 0.685), and LPL (WT-HF 1.17 ± 0.15 vs. KO-HF 1.95 ± 0.79, P = 0.685). (The amounts of PCR products were normalized with a housekeeping gene [GAPDH] to calculate the relative expression ratios.) On the other hand, the mRNA expression of LPL in adipose tissue improved in PSGL-1$^{-/-}$ mice compared with WT mice fed HFD (Fig. 5*D*). Histologically, the liver of WT mice fed HFD showed massive hepatocyte ballooning around the central veins; however, the hepatic steatosis was improved in PSGL-1$^{-/-}$ mice fed HFD (Fig. 6*C*). Furthermore, the levels of serum total cholesterol, LDL, free fatty acids, and leptin were lower in PSGL-1$^{-/-}$ mice than in WT mice fed HFD (Fig. 4*B*), but aspartate aminotransferase and alanine aminotransferase were not different between the two groups (data not shown).

DISCUSSION

To investigate the mechanism of monocytes/macrophages infiltration into adipose tissue, we used a DNA microarray

for obese adipose tissue in *db/db* mice or WT mice fed HFD. Both groups were in a state of intensive insulin resistance but were not diabetic. Expression of the adhesion molecule PSGL-1 was increased in obese adipose tissue from *db/db* mice and from WT mice fed HFD, as determined by DNA microarray analysis. In addition, an increase in PSGL-1 mRNA expression was observed with real-time RT-PCR and immunohistochemistry in obese adipose tissue. Furthermore, PSGL-1–deficient mice had reduced macrophage accumulation, insulin resistance, lipid metabolism, and steatohepatic change associated with obesity.

PSGL-1 was originally identified by expression cloning of a functional ligand for P-selectin (30). PSGL-1 is a mucin-like cell adhesion molecule expressed on the surface of leukocytes and endothelial cells and then involved in platelet-leukocyte and endothelium-leukocyte interactions. PSGL-1 mRNA was expressed in a variety of tissues, including bone marrow, brain, adipose tissue, heart, kidney, and liver. PSGL-1 is highly expressed in hematopoietic cells and in nonhematopoietic tissues, including adipose tissue and brain. The domain structure of PSGL-1 and amino acids are highly conserved between humans and rodents (31). PSGL-1 interacts with all three selectins: L-selectin (32), E-selectin (19,22), and P-selectin (29).

Earlier, it was reported that mice deficient in ICAM-1, or other leukocyte adhesion molecules, increased body weight and white fat pad weight (% of body weight) on normal food and on HFD. Mac-1 ($\alpha M\beta 2$, CD11b/CD18) is a counter-receptor for ICAM-1, and Mac-1–deficient mice showed a similar obesity phenotype (33). A1C was not different in ICAM-1–deficient *db/db* mice, streptozotocin-induced ICAM-1–deficient mice, *db/db* mice (13), and streptozotocin-induced WT mice (12). Furthermore, the number of leukocytes in the adipose tissue of ICAM-1–deficient mice and Mac-1–deficient mice fed HFD were the same as in the WT mice fed HFD. Consequently, these adhesion receptors are not required for leukocyte migration into adipose tissue (34).

In this study, PSGL-1 expression on peripheral blood monocyte was not increased in *db/db* mice compared with WT mice. Moreover, PSGL-1 expression on ATMs was also similar between *db/db* mice and WT mice by flow cytometry analysis. On the other hand, $CD31^+PSGL\text{-}1^+$ cell content was significantly increased in the SVF of eWAT in *db/db* mice compared with WT mice. These results indicate that increased expression of PSGL-1 on endothelial cells in adipose tissue is involved in infiltration of macrophage and inflammation in adipose tissue of obese mice.

The accumulation of macrophages in adipose tissue is correlated with increased body weight and insulin resistance in both humans and rodents (2,3). MCP-1 contributed to macrophage infiltration into adipose tissue and insulin resistance in mice (6,8). Those reports indicated that the ATMs might play an important role in the development of insulin resistance. Moreover, there are recent reports that the polarization of macrophages is changed from M2 to M1 in obese inflamed adipose tissue (35). M1 macrophages are induced by proinflammatory mediators such as lipopolysaccharide and γ-interferon (IFN-γ) and produce proinflammatory cytokines TNF-α and IL-6. Instead, M2 macrophages generate high levels of anti-inflammatory cytokines IL-10 and IL-1. Our data showed that MCP-1, IL-6, and iNOS mRNA levels were reduced, and IL-10 mRNA, an M2 macrophage marker, was significantly increased in eWAT from $PSGL\text{-}1^{-/-}$ mice compared with WT mice fed HFD. Whereas CD11c mRNA as an M1 macrophage marker tended to be decreased in $PSGL\text{-}1^{-/-}$ mice compared with WT mice fed HFD. These results demonstrated that PSGL-1 deficiency reduced the number of ATMs and changed the phenotype of macrophages from M1 to M2 and then affected inhibition of inflammation in eWAT. Furthermore, PSGL-1 deficiency improved insulin signaling in the muscle, as evidenced by an increase in Akt phosphorylation in animals fed HFD. As a result, $PSGL\text{-}1^{-/-}$ mice fed HFD ameliorated systemic glucose tolerance and insulin sensitivity.

Several studies reported that blockade of PSGL-1 reduced inflammatory reactions. In the model of cold ischemia/reperfusion, hepatic endothelial neutrophil infiltration and hepatocyte injury were diminished, and the expression of TNF-α, IL-6, iNOS, IL-2, and IFN-γ mRNA was decreased in livers pretreated with recombinant PSGL-Ig (36). Other reports showed that blockade of PSGL-1 attenuated macrophage recruitment in intestinal mucosa and ameliorated ileitis in a mouse model of Crohn's disease (37,38).

In this study, serum triglyceride and hepatic steatosis improved in $PSGL\text{-}1^{-/-}$ mice fed HFD. The mRNA expression of LPL was improved in adipose tissue of $PSGL\text{-}1^{-/-}$ mice compared with WT mice fed HFD. These results might be explained if the amelioration of insulin resistance increased LPL in adipose tissue. Consequently, lipid metabolism, including serum free fatty acids, triglyceride, cholesterol, and hepatic triglycerides, might be improved in $PSGL\text{-}1^{-/-}$ mice compared with WT mice fed HFD.

We found that plasma leptin levels and leptin mRNA expression in eWAT were decreased in $PSGL\text{-}1^{-/-}$ mice fed HFD, despite no difference of body weight or weight of fat. The plasma leptin concentration is positively correlated with BMI and weight of body fat in humans (39). Obese individuals are generally in a state of leptin resistance, although the pathophysiology of leptin resistance has not been clarified. Our data suggested that improvement of leptin sensitivity resulted in lower levels of plasma leptin in $PSGL\text{-}1^{-/-}$ mice than that in WT mice fed HFD. However, further studies are needed to determine whether PSGL-1 deficiency improves leptin sensitivity in obese animals.

In conclusion, our results indicate that PSGL-1 is a crucial adhesion molecule for recruitment of monocytes into adipose tissues in obese mice. PSGL-1 is a candidate for a novel therapeutic target for prevention of obesity-related insulin resistance.

ACKNOWLEDGMENTS

This study was supported in part by Grants-in-Aid for Scientific Research from the Ministry of Education, Science, Culture, Sports, and Technology of Japan.

No potential conflicts of interest relevant to this article were reported.

C.S. researched data, contributed to discussion, and wrote the manuscript. K.S. contributed to discussion and reviewed/edited the manuscript. D.H., M.S., S.N., S.M., R.K., A.T., J.W., and N.K. researched data. D.O. and H.M. reviewed/edited the manuscript. H.U.K. contributed to discussion.

We thank Dr. Kazuyuki Tobe and Dr. Shiho Fujisaka (Toyama University) for technical advice on FACS analysis.

REFERENCES

1. Wellen KE, Hotamisligil GS. Inflammation, stress, and diabetes. J Clin Invest 2005;115:1111–1119
2. Weisberg SP, McCann D, Desai M, Rosenbaum M, Leibel RL, Ferrante AW Jr. Obesity is associated with macrophage accumulation in adipose tissue. J Clin Invest 2003;112:1796–1808
3. Xu H, Barnes GT, Yang Q, Tan G, Yang D, Chou CJ, Sole J, Nichols A, Ross JS, Tartaglia LA, Chen H. Chronic inflammation in fat plays a crucial role in the development of obesity-related insulin resistance. J Clin Invest 2003;112:1821–1830
4. Hotamisligil GS, Shargill NS, Spiegelman BM. Adipose expression of tumor necrosis factor-alpha: direct role in obesity-linked insulin resistance. Science 1993;259:87–91
5. Takahashi K, Mizuarai S, Araki H, Mashiko S, Ishihara A, Kanatani A, Itadani H, Kotani H. Adiposity elevates plasma MCP-1 levels leading to the increased CD11b-positive monocytes in mice. J Biol Chem 2003;278: 46654–46660
6. Kanda H, Tateya S, Tamori Y, Kotani K, Hiasa K, Kitazawa R, Kitazawa S, Miyachi H, Maeda S, Egashira K, Kasuga M. MCP-1 contributes to macrophage infiltration into adipose tissue, insulin resistance, and hepatic steatosis in obesity. J Clin Invest 2006;116:1494–1505
7. Weisberg SP, Hunter D, Huber R, Lemieux J, Slaymaker S, Vaddi K, Charo I, Leibel RL, Ferrante AW Jr. CCR2 modulates inflammatory and metabolic effects of high-fat feeding. J Clin Invest 2006;116:115–124
8. Kamei N, Tobe K, Suzuki R, Ohsugi M, Watanabe T, Kubota N, Ohtsuka-Kowatari N, Kumagai K, Sakamoto K, Kobayashi M, Yamauchi T, Ueki K, Oishi Y, Nishimura S, Manabe I, Hashimoto H, Ohnishi Y, Ogata H, Tokuyama K, Tsunoda M, Ide T, Murakami K, Nagai R, Kadowaki T. Overexpression of monocyte chemoattractant protein-1 in adipose tissues causes macrophage recruitment and insulin resistance. J Biol Chem 2006;281:26602–26614
9. Bevilacqua MP, Nelson RM. Selectins. J Clin Invest 1993;91:379–387
10. Hirata K, Shikata K, Matsuda M, Akiyama K, Sugimoto H, Kushiro M, Makino H. Increased expression of selectins in kidneys of patients with diabetic nephropathy. Diabetologia 1998;41:185–192
11. Sugimoto H, Shikata K, Hirata K, Akiyama K, Matsuda M, Kushiro M, Shikata Y, Miyatake N, Miyasaka M, Makino H. Increased expression of intercellular adhesion molecule-1 (ICAM-1) in diabetic rat glomeruli: glomerular hyperfiltration is a potential mechanism of ICAM-1 upregulation. Diabetes 1997;46:2075–2081
12. Okada S, Shikata K, Matsuda M, Ogawa D, Usui H, Kido Y, Nagase R, Wada J, Shikata Y, Makino H. Intercellular adhesion molecule-1-deficient mice are resistant against renal injury after induction of diabetes. Diabetes 2003;52:2586–2593
13. Chow FY, Nikolic-Paterson DJ, Ozols E, Atkins RC, Tesch GH. Intercellular adhesion molecule-1 deficiency is protective against nephropathy in type 2 diabetic db/db mice. J Am Soc Nephrol 2005;16:1711–1722
14. Leinonen E, Hurt-Camejo E, Wiklund O, Hulten LM, Hiukka A, Taskinen MR. Insulin resistance and adiposity correlate with acute-phase reaction and soluble cell adhesion molecules in type 2 diabetes. Atherosclerosis 2003;166:387–394
15. Targher G, Bonadonna RC, Alberiche M, Zenere MB, Muggeo M, Bonora E. Relation between soluble adhesion molecules and insulin sensitivity in type 2 diabetic individuals: role of adipose tissue. Diabetes Care 2001;24: 1961–1966
16. Straczkowski M, Lewczuk P, Dzienis-Straczkowska S, Kowalska I, Stepien A, Kinalska I. Elevated soluble intercellular adhesion molecule-1 levels in obesity: relationship to insulin resistance and tumor necrosis factor-alpha system activity. Metabolism 2002;51:75–78
17. Troseid M, Lappegard KT, Mollnes TE, Arnesen H, Seljeflot I. Changes in serum levels of E-selectin correlate to improved glycaemic control and reduced obesity in subjects with the metabolic syndrome. Scand J Clin Lab Invest 2005;65:283–290
18. Couillard C, Ruel G, Archer WR, Pomerleau S, Bergeron J, Couture P, Lamarche B, Bergeron N. Circulating levels of oxidative stress markers and endothelial adhesion molecules in men with abdominal obesity. J Clin Endocrinol Metab 2005;90:6454–6459
19. Xia L, Sperandio M, Yago T, McDaniel JM, Cummings RD, Pearson-White S, Ley K, McEver RP. P-selectin glycoprotein ligand-1-deficient mice have impaired leukocyte tethering to E-selectin under flow. J Clin Invest 2002;109:939–950
20. Yang J, Hirata T, Croce K, Merrill-Skoloff G, Tchernychev B, Williams E, Flaumenhaft R, Furie BC, Furie B. Targeted gene disruption demonstrates that P-selectin glycoprotein ligand 1 (PSGL-1) is required for P-selectin-mediated but not E-selectin-mediated neutrophil rolling and migration. J Exp Med 1999;190:1769–1782
21. Dennis G Jr, Sherman BT, Hosack DA, Yang J, Gao W, Lane HC, Lempicki RA. DAVID: Database for Annotation, Visualization, and Integrated Discovery. Genome Biol 2003;4:P3
22. Hirata T, Merrill-Skoloff G, Aab M, Yang J, Furie BC, Furie B. P-Selectin glycoprotein ligand 1 (PSGL-1) is a physiological ligand for E-selectin in mediating T helper 1 lymphocyte migration. J Exp Med 2000;192:1669–1676
23. Joost HG, Schurmann A. Subcellular fractionation of adipocytes and 3T3–L1 cells. Methods Mol Biol 2001;155:77–82
24. Eguchi J, Wada J, Hida K, Zhang H, Matsuoka T, Baba M, Hashimoto I, Shikata K, Ogawa N, Makino H. Identification of adipocyte adhesion molecule (ACAM), a novel CTX gene family, implicated in adipocyte maturation and development of obesity. Biochem J 2005;387:343–353
25. Ogawa D, Shikata K, Honke K, Sato S, Matsuda M, Nagase R, Tone A, Okada S, Usui H, Wada J, Miyasaka M, Kawashima H, Suzuki Y, Suzuki T, Taniguchi N, Hirahara Y, Tadano-Aritomi K, Ishizuka I, Tedder TF, Makino H. Cerebroside sulfotransferase deficiency ameliorates L-selectin-dependent monocyte infiltration in the kidney after ureteral obstruction. J Biol Chem 2004;279:2085–2090
26. Folch J, Lees M, Sloane Stanley GH. A simple method for the isolation and purification of total lipids from animal tissues. J Biol Chem 1957;226:497–509
27. Hicks AE, Nolan SL, Ridger VC, Hellewell PG, Norman KE. Recombinant P-selectin glycoprotein ligand-1 directly inhibits leukocyte rolling by all 3 selectins in vivo: complete inhibition of rolling is not required for anti-inflammatory effect. Blood 2003;101:3249–3256
28. Norman KE, Katopodis AG, Thoma G, Kolbinger F, Hicks AE, Cotter MJ, Pockley AG, Hellewell PG. P-selectin glycoprotein ligand-1 supports rolling on E- and P-selectin in vivo. Blood 2000;96:3585–3591
29. Yang J, Furie BC, Furie B. The biology of P-selectin glycoprotein ligand-1: its role as a selectin counterreceptor in leukocyte-endothelial and leukocyte-platelet interaction. Thromb Haemost 1999;81:1–7
30. Sako D, Chang XJ, Barone KM, Vachino G, White HM, Shaw G, Veldman GM, Bean KM, Ahern TJ, Furie B, et al. Expression cloning of a functional glycoprotein ligand for P-selectin. Cell 1993;75:1179–1186
31. Yang J, Galipeau J, Kozak CA, Furie BC, Furie B. Mouse P-selectin glycoprotein ligand-1: molecular cloning, chromosomal localization, and expression of a functional P-selectin receptor. Blood 1996;87:4176–4186
32. McEver RP, Cummings RD. Role of PSGL-1 binding to selectins in leukocyte recruitment. J Clin Invest 1997;100:S97–S103
33. Dong ZM, Gutierrez-Ramos JC, Coxon A, Mayadas TN, Wagner DD. A new class of obesity genes encodes leukocyte adhesion receptors. Proc Natl Acad Sci U S A 1997;94:7526–7530
34. Robker RL, Collins RG, Beaudet AL, Mersmann HJ, Smith CW. Leukocyte migration in adipose tissue of mice null for ICAM-1 and Mac-1 adhesion receptors. Obes Res 2004;12:936–940
35. Lumeng CN, Bodzin JL, Saltiel AR. Obesity induces a phenotypic switch in adipose tissue macrophage polarization. J Clin Invest 2007;117:175–184
36. Amersi F, Farmer DG, Shaw GD, Kato H, Coito AJ, Kaldas F, Zhao D, Lassman CR, Melinek J, Ma J, Volk HD, Kupiec-Weglinski JW, Busuttil RW. P-selectin glycoprotein ligand-1 (rPSGL-Ig)-mediated blockade of CD62 selectin molecules protects rat steatotic liver grafts from ischemia/reperfusion injury. Am J Transplant 2002;2:600–608
37. Inoue T, Tsuzuki Y, Matsuzaki K, Matsunaga H, Miyazaki J, Hokari R, Okada Y, Kawaguchi A, Nagao S, Itoh K, Matsumoto S, Miura S. Blockade of PSGL-1 attenuates CD14+ monocytic cell recruitment in intestinal mucosa and ameliorates ileitis in SAMP1/Yit mice. J Leukoc Biol 2005;77: 287–295
38. Rivera-Nieves J, Burcin TL, Olson TS, Morris MA, McDuffie M, Cominelli F, Ley K. Critical role of endothelial P-selectin glycoprotein ligand 1 in chronic murine ileitis. J Exp Med 2006;203:907–917
39. Hosoda K, Masuzaki H, Ogawa Y, Miyawaki T, Hiraoka J, Hanaoka I, Yasuno A, Nomura T, Fujisawa Y, Yoshimasa Y, Nishi S, Yamori Y, Nakao K. Development of radioimmunoassay for human leptin. Biochem Biophys Res Commun 1996;221:234–239

Clin Exp Nephrol
DOI 10.1007/s10157-010-0357-1

ORIGINAL ARTICLE

Renoprotective effects of clarithromycin via reduction of urinary MCP-1 levels in type 2 diabetic patients

Atsuhito Tone · Kenichi Shikata · Koichi Nakagawa · Masaaki Hashimoto · Hirofumi Makino

Received: 5 July 2010 / Accepted: 19 September 2010

Abstract
Background Recent studies have shown the involvement of microinflammation in the pathogenesis of diabetic nephropathy. We previously demonstrated that erythromycin, one of the macrolides, ameliorated renal injury via anti-inflammatory effects in experimental diabetic rats. We conducted an open randomized controlled pilot study to investigate the renoprotective effect of clarithromycin for diabetic nephropathy in type 2 diabetic patients manifesting albuminuria.
Methods Sixteen patients were randomly assigned to the control ($n = 8$) or the CAM group in which they received 200 mg/day of clarithromycin ($n = 8$). At the beginning of the study and after 3 months of investigation, the following parameters were assessed: urinary albumin creatinine ratio (ACR), the levels of serum MCP-1, soluble ICAM-1, IL-18, IL-6 and hs-CRP, and the levels of urinary MCP-1 and IL-18.
Results The changes in urinary ACR were significantly improved ($P = 0.039$), and serum creatinine levels showed a decreasing trend ($P = 0.053$) in the CAM group compared with the control group. Urinary MCP-1 levels were significantly reduced in the clarithromycin-administrated group ($P = 0.009$). However, there was no significant difference in other proinflammatory markers. A significant positive correlation was obtained between the post-to-pre-urinary ACR and the post-to-pre-urinary MCP-1 ratio($r = 0.526$, $P = 0.043$). In the CAM group, the changes of serum creatinine also showed a significant positive correlation with those of urinary ACR, urinary MCP-1, urinary IL-18 and serum levels of soluble ICAM-1.
Conclusion The results from our study suggest that clarithromycin may attenuate the production of renal MCP-1 in type 2 diabetic patients, resulting in amelioration of urinary ACR via anti-inflammatory effects. Modulation of microinflammation with clarithromycin may provide a new approach for diabetic nephropathy.

Keywords Diabetic nephropathy · Clarithromycin · MCP-1 · Microinflammation · Macrolide

A. Tone (✉)
Department of Diabetes and Metabolism,
National Hospital Organization, Okayama Medical Center,
1711-1 Tamasu, Kita-ku, Okayama 701-1192, Japan
e-mail: aitone@okayama3.hosp.go.jp

K. Shikata · H. Makino
Department of Medicine and Clinical Science,
Okayama University Graduate School of Medicine,
Dentistry and Pharmaceutical Sciences, Okayama, Japan

K. Nakagawa · M. Hashimoto
Department of Surgery,
Fukuyama Daiichi Hospital, Fukuyama, Japan

Introduction

Diabetic nephropathy is a major cause of end-stage renal disease (ESRD) worldwide. It is well known that the tissue renin-angiotensin system (RAS) is activated in the kidneys of diabetic patients and that angiotensin-converting enzyme inhibitors (ACEI) and angiotensin II type 1 receptor antagonists (ARB) play central roles in the therapy for diabetic nephropathy [1, 2]. However, there is no established therapy following ACEI and ARB at present, and additional therapeutic strategies for diabetic nephropathy are needed.

Published online: 03 November 2010

Several mechanisms contribute to the development of diabetic nephropathy, such as glomerular hyperfiltration [3], activation of protein kinase C (PKC) [4] and accumulation of advanced glycation end-products (AGEs) [5, 6]. In addition to these pathways, recent studies have shown that inflammatory mechanisms are involved in the pathogenesis of diabetic nephropathy. Macrophages have been reported to infiltrate into the renal tissues and glomerular and interstitial injury to be associated with macrophage infiltration in diabetic nephropathy [7–9]. Monocyte chemoattractant protein-1 (MCP-1), one of the chemokines inducing macrophage migration to the lesion, is upregulated in diabetic nephropathy [10]. Renal MCP-1 is synthesized in the tubular epithelial cells via nuclear factor-kappa B (NF-κB) activation [11, 12] and recruits monocytes/macrophages into the glomeruli and interstitinum, resulting in glomerular and tubulointerstitial inflammation, tubular atrophy and interstitial fibrosis [11, 13].

On the other hand, it is well known that 14-membered ring macrolide antibiotics have anti-inflammatory effects as well as antibacterial effects in the fields of respiratory medicine and otolaryngology. Low-dose and long-term therapy with macrolides is effective for chronic obstructive pulmonary disease (COPD), diffuse panbronchiolitis (DPB) and chronic sinusitis by reduction of intercellular adhesion molecule-1 (ICAM-1) expression or NF-κB activation in the airway epithelial cells [14, 15].

Based on these findings, we previously demonstrated that erythromycin, one of the macrolide antibiotics, ameliorated renal injury through suppression of renal NF-κB activation and macrophage infiltration into the renal tissues in experimental diabetic rats [16]. Here, we report the open randomized controlled pilot study of clarithromycin, one of the macrolides, for diabetic nephropathy in patients with type 2 diabetes. In this study, we enrolled type 2 diabetic patients manifesting persistent albuminuria, and assessed the effects of clarithromycin on urinary albumin creatinine ratio (ACR) and proinflammatory markers such as urinary MCP-1 and IL-18, serum MCP-1, soluble ICAM-1, IL-18, IL-6 and hypersensitive C-reactive protein (hs-CRP).

Patients and methods

Sixteen patients with type 2 diabetes mellitus and diabetic nephropathy manifesting persistent albuminuria (100–500 mg/g Cr) were enrolled. They were randomly assigned to the control group ($n = 8$) or the CAM group ($n = 8$). Patients in the CAM group received 200 mg of clarithromycin at a single daily dose for 3 months. At the beginning of the study and after 3 months of the investigational period, the following parameters were assessed: blood pressure, body weight, HbA1c, serum creatinine, creatinine clearance (Ccr), urinary ACR, the levels of serum MCP-1, soluble ICAM-1, IL-18, IL-6 and hs-CRP, and the levels of urinary MCP-1 and IL-18. Dipstick tests for white blood cells (WBC) were also performed to rule out urinary tract infection. Venous blood and urine samples were obtained in the early morning after overnight fasting. Ccr was calculated by the Cockcroft-Gault formula. Diabetic nephropathy was diagnosed clinically if the following criteria were fulfilled: persistent albuminuria, presence of diabetic retinopathy, and no clinical or laboratory evidence of non-diabetic renal diseases.

Of all participants, 8 patients received insulin therapy, and the remaining 8 received oral antidiabetic agents. Thirteen patients (6 patients in the control group and 7 patients in the CAM group) had hypertension, defined as systolic blood pressure (SBP) >140 mmHg and/or diastolic blood pressure (DBP) >90 mmHg, or as being administered of one or more antihypertensive agents. Nine patients (4 patients in the control group and 5 patients in the CAM group) had treatment with ACEI and/or ARB at the start of the study. Start or withdrawal of administration of ACEI/ARB, or changing a dose of ACEI/ARB did not occur throughout the 3 months of the study.

Informed consent was obtained from all participants, and the study protocol was approved by the ethics committee of Fukuyama Daiichi Hospital.

Measurement of proinflammatory markers

Serum levels of hs-CRP were measured using an immunonephelometric assay kit (Dade Behring, Marburg, Germany). The levels of MCP-1, soluble ICAM-1, IL-18 and IL-6 were measured with an ELISA kit (Quantikine; R&D Systems, Minneapolis, MN). For hs-CRP concentrations, the intra-assay coefficient of variance (CV) was 1.7% at 194.6 ng/ml and 0.9% at 1178 ng/ml, and equivalent inter-assay CVs were 3.0 and 2.3%, respectively. For MCP-1 concentrations, the intra-assay CVs were 7.8 and 4.7% at 76.7 and 364 pg/ml, and equivalent inter-assay CVs were 6.7 and 5.8%, respectively. For soluble ICAM-1 concentrations, the intra-assay CV was 7.9% at 167.6 ng/ml and 6.5% at 312.4 ng/ml, and equivalent inter-assay CVs were 7.6 and 11.6%, respectively. For IL-18 concentrations, the intra-assay CVs were 5.6 and 4.9% at 136.1 and 600.7 pg/ml, and equivalent inter-assay CVs were 6.3 and 5.2%, respectively. For IL-6 concentrations, the intra-assay CV was 4.7% at 3.72 pg/ml and 4.6% at 20.5 pg/ml, and equivalent inter-assay CVs were 3.6 and 6.4%, respectively.

Exclusion criteria

To rule out pre-existing infections, we excluded the patients with clinical symtoms of a common cold, upper respiratory inflammation, gastroenteritis and urinary-tract

Table 1 Characteristics of the patients and changes in clinical parameters at baseline and after 3 months of the investigation

	Control ($n = 8$)			CAM ($n = 8$)			P^a	P^b
	Baseline	3 months	P	Baseline	3 months	P		
Gender (male/female)	5/3	–	–	7/1	–	–	0.248	–
Age (years)	65.8 ± 3.0	–	–	68.3 ± 3.8	–	–	0.609	–
Duration of diabetes (years)	15.0 ± 2.3	–	–	19.8 ± 4.6	–	–	0.370	–
BMI (kg/m^2)	23.6 ± 1.80	–	–	24.4 ± 1.5	–	–	0.754	–
SBP (mmHg)	134 ± 6	131 ± 8	0.486	128 ± 6	138 ± 7	0.071	0.512	–
DBP (mmHg)	75 ± 5	72 ± 4	0.486	69 ± 4	72 ± 4	0.392	0.373	–
HbA1c (%)	8.1 ± 0.5	8.2 ± 0.6	0.548	7.9 ± 0.5	7.8 ± 0.5	0.801	0.870	–
Serum creatinine (mg/dl)	0.83 ± 0.09	0.83 ± 0.09	–	0.94 ± 0.11	0.85 ± 0.11	0.053	0.434	–
Creatinine clearance (ml/min)	78.3 ± 11.1	78.7 ± 11.4	0.953	76.7 ± 13.5	90.1 ± 19.4	0.121	0.927	–
Urinary ACR (mg/g Cr)	168 ± 30	221 ± 53	0.123	191 ± 34	159 ± 31	0.138	0.477	–
ΔuACR (mg/g Cr)	78 ± 44			−32 ± 19				0.039†
Use of ACEI and/or ARB	4	4	–	5	5	–	0.614	–
Use of statin	5	5	–	3	3	–	0.317	–

P value by the paired t test or Wilcoxon signed-rank test. Data are expressed as mean ± SEM. Data on sex, use of ACEI and/or ARB, and use of statin are given as the frequency

† $P < 0.05$

[a] P values for comparison at the start of the study between the control and CAM groups by Student's unpaired t test or χ^2 test (sex, use of ACEI and/or ARB, and use of statin)

[b] P values for comparison in changes between the control and CAM groups by Student's unpaired t test

infection. We also excluded the patients with a high hs-CRP level of more than 4000 ng/ml.

Statistical analysis

Statistical analyses were processed using the Stat View J-5.0 software package (SAS Institute Inc., Cary, NC) and SPSS Statistics 18 (SPSS Inc., IBM Company Headquarters, Chicago, IL). Data are expressed as the mean ± SEM. For comparison at the start of the study between the control and CAM groups, Student's unpaired t test or χ^2 test (gender, use of ACEI and/or ARB, and use of statin) were used. Data for the two measurement time points for each individual were compared by the paired t test and Wilcoxon signed-rank test. Comparison of changes between the control and CAM groups was assessed with Student's unpaired t test. For correlational analysis between the changes of urinary ACR or serum creatinine and those of proinflammatory markers, Pearson's correlation coefficients were used. Multiple linear regression analysis was used to analyze the relationship between urinary ACR and proinflammatory markers. A P value less than 0.05 was regarded as statistically significant.

Results

There were no adverse effects of clarithromycin in the intervention period. The results of dipstick tests for WBC were negative both at the start and the end of the study in 15 patients. In one female patient of the control group, the result of dipstick tests for WBC was suspicious (+/−) at the baseline and positive (1+) at the end of the study.

Characteristics of the patients and changes in urinary ACR are presented in Table 1. Clinical characteristics and laboratory data at baseline did not significantly differ between the Control and CAM groups. SBP, DBP, HbA1c and Ccr were statistically unchanged throughout the 3 months of the study. Serum creatinine levels showed a decreasing trend in the CAM group, though they were not statistically significant. Urinary ACR showed a decrease in the CAM group, and there was a significant difference between the changes in urinary ACR (ΔuACR) of the control and the CAM group ($P = 0.039$).

The changes in proinflammatory markers were shown in Fig. 1. In the CAM group, urinary MCP-1 levels were significantly reduced after 3 months of the study compared with the baseline ($P = 0.009$, Fig. 1b). However, there was no significant difference in serum MCP-1, soluble ICAM-1, IL-18, hs-CRP, IL-6 and urinary IL-18 (Fig. 1a, c–g).

A significant positive correlation was obtained between the urinary ACR and urinary MCP-1 ratios (calculated as the value of each variable after 3 months divided by the respective value at baseline) ($r = 0.526$, $P = 0.043$, Fig. 2). In the CAM group, the changes of serum creatinine levels showed a significant positive correlation with those of urinary ACR, urinary MCP-1, urinary IL-18 and serum levels of soluble ICAM-1 levels (Fig. 3a–d).

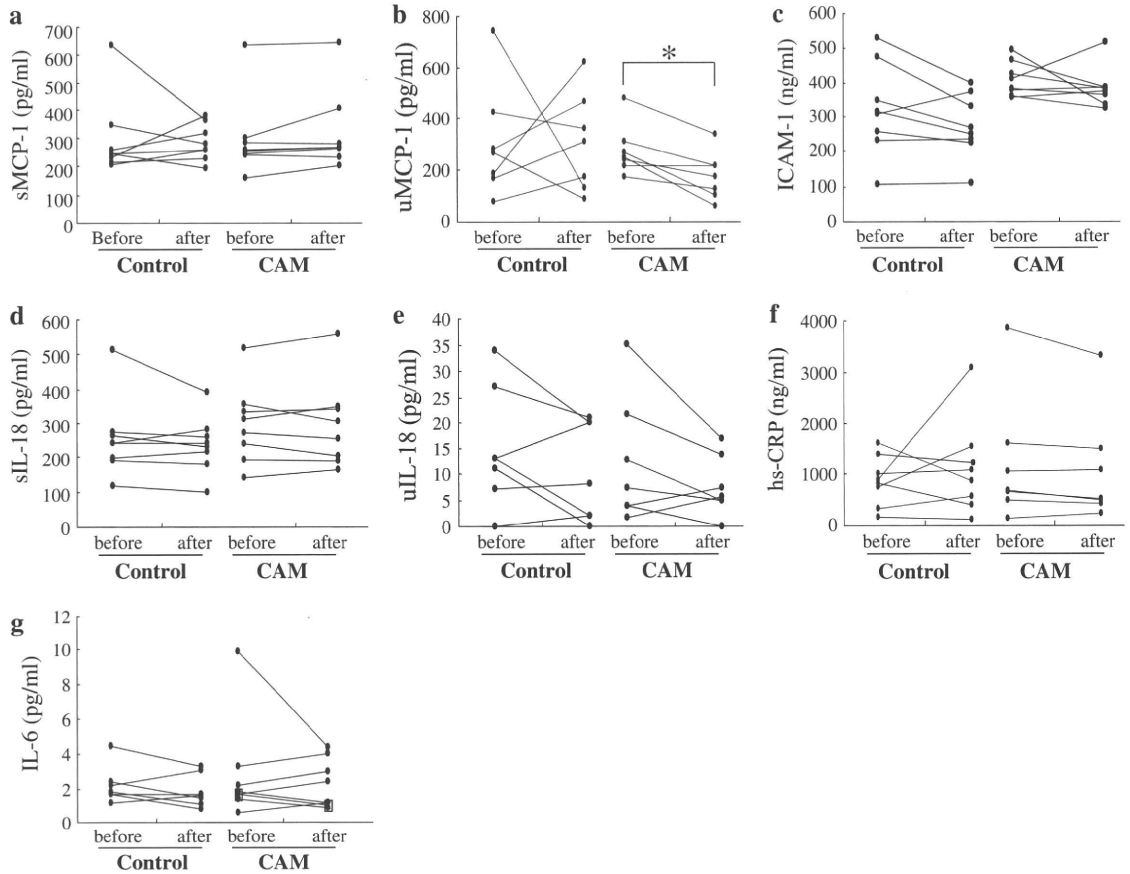

Fig. 1 The changes in serum MCP-1 (**a**), urinary MCP-1 (**b**), serum soluble ICAM-1 (**c**), serum IL-18 (**d**), urinary IL-18 (**e**), serum hs-CRP (**f**) and serum IL-6 (**g**). $*P < 0.01$

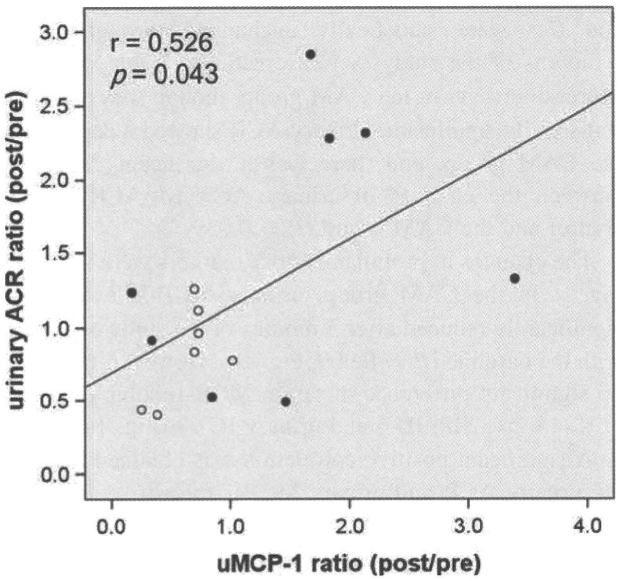

Fig. 2 Correlation between the urinary ACR and urinary MCP-1 ratios. *Filled circles* Control group; *open circles* CAM group

To determine independent associations between urinary ACR and proinflammatory markers at the baseline, multiple linear regression analysis was performed with the urinary ACR as the dependent variable and proinflammatory markers as independent variables. As a result, urinary MCP-1 and soluble ICAM-1 were significantly associated with urinary ACR (Table 2).

Discussion

In this study, we found that urinary MCP-1 levels were significantly reduced in patients treated with clarithromycin. The changes in urinary ACR were improved in the CAM group compared with the control group with a significant difference without changes in glycemic control or blood pressure. Furthermore, the changes in urinary ACR showed a significant positive correlation with those of urinary MCP-1 levels. On the other hand, serum creatinine levels showed a decreasing trend in the CAM group, and